ADVANCED ENERGY & SUSTAINABILITY RESEARCH
www.advenergysustres.com

A Review on Ceo_2-Based Electrocatalyst and Photocatalyst in Energy Conversion

Qingqing Li, Lianpeng Song, Zhong Liang, Mingzi Sun, Tong Wu, Bolong Huang, Feng Luo, Yaping Du,* and Chun-Hua Yan*

The activation and conversion of small molecules (H_2, O_2, H_2O, CO_2, N_2, CH_3OH, and C_2H_5OH) in energy-related systems has attracted researchers' attentions around the world. The conversion of these molecules plays a key role in renewable energy storage and conversion systems, and for that, the electrocatalysis and photocatalysis processes are considered as clean and efficient strategies. Numerous materials are designed to promote the conversion process to satisfy the different requirements for efficiency and selectivity. Due to the flexible switching between Ce^{3+} and Ce^{4+} with rich oxygen defects, CeO_2-based materials display excellent performance in all the related reaction processes. Herein, the CeO_2-based electro(photo)catalysts according to different reactions are summarized. Specifically, the influence of material compositions, morphologies, and structures on catalytic performance is discussed, and the significant role of CeO_2 is emphasized. Finally, several approaches are advocated to promote the development of CeO_2-based electro(photo)catalysis and accelerate their industrial application.

1. Introduction

With the increasing energy demands and the impending climate change, the researchers have to turn their attention to develop sustainable and clean pathways to produce fuels and chemicals. Creating a global-scale sustainable energy system for the future to preserve our environment is one of the most crucial challenges facing humanity today.[1] High-efficiency conversion of electrical energy from renewable energy sources (such as wind energy, solar energy, etc.) into chemical energy is an effective strategy for making full use of and storing energy.[2] Reducing carbon dioxide relieves the greenhouse effect and provides the chemical feedstocks through a carbon recycle (carbon monoxide, formate, formaldehyde, methane, methanol, methanol, and C_{2+} hydrocarbons and oxygenates).[3] Water splitting, which comprises two half-cell reactions, can provide us with clean hydrogen as fuel.[4] Fuel cell is a type of environmental friendly energy-conversion device with two half-reactions as oxygen reaction and fuel oxidation.[5] In addition, nitrogen reduction reaction can convert the dinitrogen molecules in the atmosphere into ammonia, a higher-value product.[6] To cleanly and sustainably realize the activation and efficient conversion of the above energy molecules, one prospective goal is to develop electrochemical and photochemical process. The key to enable this vision is the development of improved electrocatalysts and photocatalysts with high efficiency and selectivity for the energy molecules transformations involved.[2] A number of catalysts have been developed for the related reaction such as hydrogen evolution reaction (HER),[7] hydrogen oxidation reaction,[8] oxygen evolution reaction (OER),[8] oxygen reduction reaction (ORR),[9] methanol/ethanol oxidation reaction (M/EOR),[10] carbon dioxide reduction reaction (CO_2RR), and nitrogen reduction reaction (NRR).[11] Currently, the IrO_2, RuO_2, and Pt/C are the benchmarking electrocatalysts for these catalytic processes; however, the scarcity and high cost of these materials limit its wide applications. Although various metal-based, metal oxide-based, and

Q. Li, L. Song, Z. Liang, Prof. F. Luo, Prof. Y. Du, Prof. C.-H. Yan
Tianjin Key Lab for Rare Earth Materials and Applications
Center for Rare Earth and Inorganic Functional Materials
School of Materials Science and Engineering
National Institute for Advanced Materials
Nankai University
Tianjin 300350, China
E-mail: ypdu@nankai.edu.cn

The ORCID identification number(s) for the author(s) of this article can be found under https://doi.org/10.1002/aesr.202000063.

© 2021 The Authors. Advanced Energy and Sustainability Research published by Wiley-VCH GmbH. This is an open access article under the terms of the Creative Commons Attribution License, which permits use, distribution and reproduction in any medium, provided the original work is properly cited.

DOI: 10.1002/aesr.202000063

M. Sun, T. Wu, Prof. B. Huang
Department of Applied Biology and Chemical Technology
The Hong Kong Polytechnic University
Hung Hom, Kowloon, Hong Kong SAR, China
E-mail: bhuang@polyu.edu.hk

Prof. C.-H. Yan
Beijing National Laboratory for Molecular Sciences
State Key Laboratory of Rare Earth Materials Chemistry and Applications
PKU-HKU Joint Laboratory in Rare Earth Materials and Bioinorganic Chemistry
College of Chemistry and Molecular Engineering
Peking University
Beijing, China

Prof. C.-H. Yan
College of Chemistry and Chemical Engineering
Lanzhou University
Lanzhou 730000, China

 © 2021 The Authors. Advanced Energy and Sustainability Research published by Wiley-VCH GmbH

carbon-based catalysts have been extensively studied, there is still room for further improvement in their activity, stability, and cost. A number of photocatalysts also have been designed and researched; however, the conversion efficiency of light to chemical energy and the selectivity for targeted products are far from satisfactory hitherto. It is worth noting that, in the development of high-efficient electrocatalysts and photocatalysts, CeO_2 plays an important role in enhancing the catalytic performance due to its unique physical and chemical properties.[12–15]

CeO_2, a rare earth oxide widely studied, has shined in thermocatalysis, electrocatalysis, and photocatalysis (**Scheme 1**). CeO_2 nanocrystal has the fluorite crystal structure with space group *Fm3m* and the cell parameters of 0.5411 nm ($a = b = c$). In the CeO_2 unit cell, each Ce^{4+} is coordinated with eight adjacent O^{2-} to form an octahedral interstitial, and each O^{2-} is coordinated with four adjacent Ce^{4+} to form a tetrahedral unit.[16] The unfilled 4f orbital and abundant electronic energy levels endow CeO_2 to have a great potential in catalysis. The electronic structure of Ce is [Xe] $4f^1 5d^1 6s^2$, where Ce^{3+} and Ce^{4+} are able to exist steadily and convert to each other easily. The multivalence property of CeO_2 will offer the opportunity to generate strong interactions with other components in catalysts and thereby enhance the performance of electrocatalysts and photocatalysts.[17] In addition, the unique crystal structure and reversible valence characteristics of CeO_2 enable the formation of oxygen vacancies to generate a defect-rich structure, which determines the excellent catalytic performance. Oxygen vacancy, derived from Ce^{4+} to Ce^{3+} reduction conversion or lattice oxygen migration, has a great influence on the electronic and chemical properties of CeO_2. In the catalysts, oxygen vacancy not only anchors active component nanoparticles or clusters but also regulates the electronic structure of catalysts.[18] It also has impact on the bandgap, light-harvesting, and electron–hole pair recombination of catalysts, which closely related to photocatalytic activity. Moreover, the high stability of CeO_2 in both acidic and alkaline environments is also favored to electrocatalytic process. Based on the unique physical and chemical properties of CeO_2, tuning the size, structure, and exposed crystal planes is a promising strategy to construct the high-efficient CeO_2-based electrocatalysts and photocatalysts. This field is developing rapidly and a timely review on both electrocatalysts and photocatalysts in energy conversion is great of meaningful.

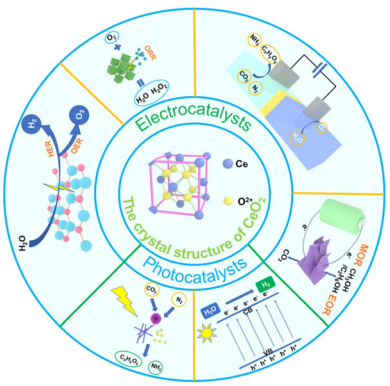

Scheme 1. Illustration of CeO_2-based electro(photo)catalysts in energy-related small molecules conversion.

2. CeO_2-Based Electrocatalyst

2.1. Hydrogen Evolution Reaction

In response to the rapid depletion of fossil fuel and growing environmental problem issues, researchers have turned their attention to the clean molecular hydrogen energy, which is usually generated by the water splitting effectively and conveniently. As a half reaction of water splitting, HER is a two-electron transfer reaction and generally involves the Volmer–Tafel path or the Volmer–Heyrovsky path. To achieve large-scale industrial hydrogen production, highly active catalysts are required to lower the overpotential for HER. Due to the strong electronic interactions, CeO_2 usually has a strong electronic interaction with other materials and then regulate their electronic structure, so it often is chosen to be support or other key component to fabricate HER catalysts. Due to the poor conductivity of CeO_2, the strategy of compositing CeO_2 with highly conductive materials is often used to enhance the activity of CeO_2-based electrocatalysts.

Liu et al. constructed 3D reduced graphene supported CeO_2 hollow microspheres by a hydrothermal self-assembly method to catalyze HER.[19] Enhanced activities with low onset overpotential of 192 mV and overpotential of 340 mV at a current density of 10 mA cm^{-2} are achieved due to the highly conductive network and rich porous structure on 3D reduced graphene. Novel metal catalysts usually have high catalytic activity, and the activity will be improved if combined with a suitable support. Gao et al. fabricated sub-nanometer Pd clusters confined in porous CeO_2 and the electrochemical results of the obtained catalysts show nearly 100 times higher activity HER than Pt/C catalyst at low-potential region.[20] The adsorption state of H* on the Pd cluster is effectively modulated by the electron transfer between Pd and O atoms, and then, the conjoint effect promotes the HER catalytic activity.

Another work by Gao et al. reached similar conclusions, where the electron transfer from Pd to CeO_2 leads to oxidized Pd and formation of Pd–O–Ce structure, which provides a new catalytic active site for HER.[21] Rh^0/CeO_2 and Ru^0/CeO_2 catalysts were also prepared for HER, which both have exceptional durability in an acidic environment for over 10 000 scans.[22,23] These results indicated that CeO_2 not only plays as an activity enhancer but also as a catalyst stabilizer. In addition to novel metal catalysts, nonprecious metal-based catalysts such as 3d transition metals Fe, Co, and Ni also have good catalytic performances for HER. The 3D porous Ni/CeO_2 nanosheet array supported on Ti mesh was prepared by Sun et al. to boosting HER for both high catalytic activity and good durability were achieved.[24] Xiao et al. encapsulated different transition metals M (M = Fe, Co, and Ni) in carbon nanotubes and then supported with CeO_2 support ($M@CNT/CeO_2$) to compare the catalytic activity of Fe, Co, and Ni for HER.[25] The results showed that the Co has a much higher activity for HER than Fe and Ni in $M@CNT/CeO_2$, which is consistent with density functional theory (DFT) calculation results. Most recently, Kang et al. prepared Co-doped CeO_2 nanosheets by a thermal decomposition exfoliation method. The introduction of Co atoms doped into CeO_2 crystal lattice generated more oxygen vacancies, which enable the fast water dissociation. As a result, the high surface, optimized hydrogen adsorption and

© 2021 The Authors. Advanced Energy and Sustainability Research published by Wiley-VCH GmbH

oxygen vacancies coordinatively contributed to the Co-doped CeO_2 as an efficient HER catalysts.[26]

Transition metal phosphides have been studied for HER catalysts, and especially CoP has received the most attention. Xiong et al. fabricated nanohybid CeO_2–CoP–C catalyst by a co-ionic-exchange and low-temperature phosphorization method.[27] The CeO_2–CoP–C catalyst displayed an obvious enhancement in catalytic performance for HER compared to the CoP–C catalyst due to the synergistic reaction between CeO_2 and CoP. The synergistic reaction not only decreases the hydrogen absorption energy to promote gas escape but also optimizes the electronic structure of catalyst to more favorable for HER. In addition, a CoP/CeO_2 interface was built to promote HER and DFT indicated that a lower water splitting energy barrier and more optimized hydrogen adsorption free energy are achieved compared to CoP by constructing CoP/CeO_2 interface (**Figure 1**a–c).[28] Similarly, the Ni_2P–CeO_2 interface was also fabricated and, as expected, has an enhanced HER activity (Figure 1d–f).[29] Moreover, Ni_3N and Ni–S alloys, etc., were composited to CeO_2 and both generate good electrocatalytic properties (Figure 1g–i).[30–32] Therefore, the HER activity and stability of different catalysts including novel metal, transition metals, transition metal phosphides, and transition metal nitrides catalysts are enhanced by compositing CeO_2 since it tends to regulate and optimize the electronic structure of catalyst (**Table 1**). The optimized hydrogen adsorption free energy caused by adjusting the electronic structure of catalysts leads to a promoted HER performance.

2.2. Hydrogen Oxidation Reaction

Compared to proton exchange membrane fuel cells (PEMFCs), anion exchange membrane fuel cells (AEMFCs) catch more eyes due to the development of platinum group metal-free electrocatalysts. However, the sluggish kinetics of hydrogen oxidation reaction (HOR) in alkaline media and poor stability have impeded AEMFC development, so rational design and fabrication of highly active electrocatalysts to enhance HOR is of great significance. Bellini et al. construct Pd–CeO_2/C to replace Pt

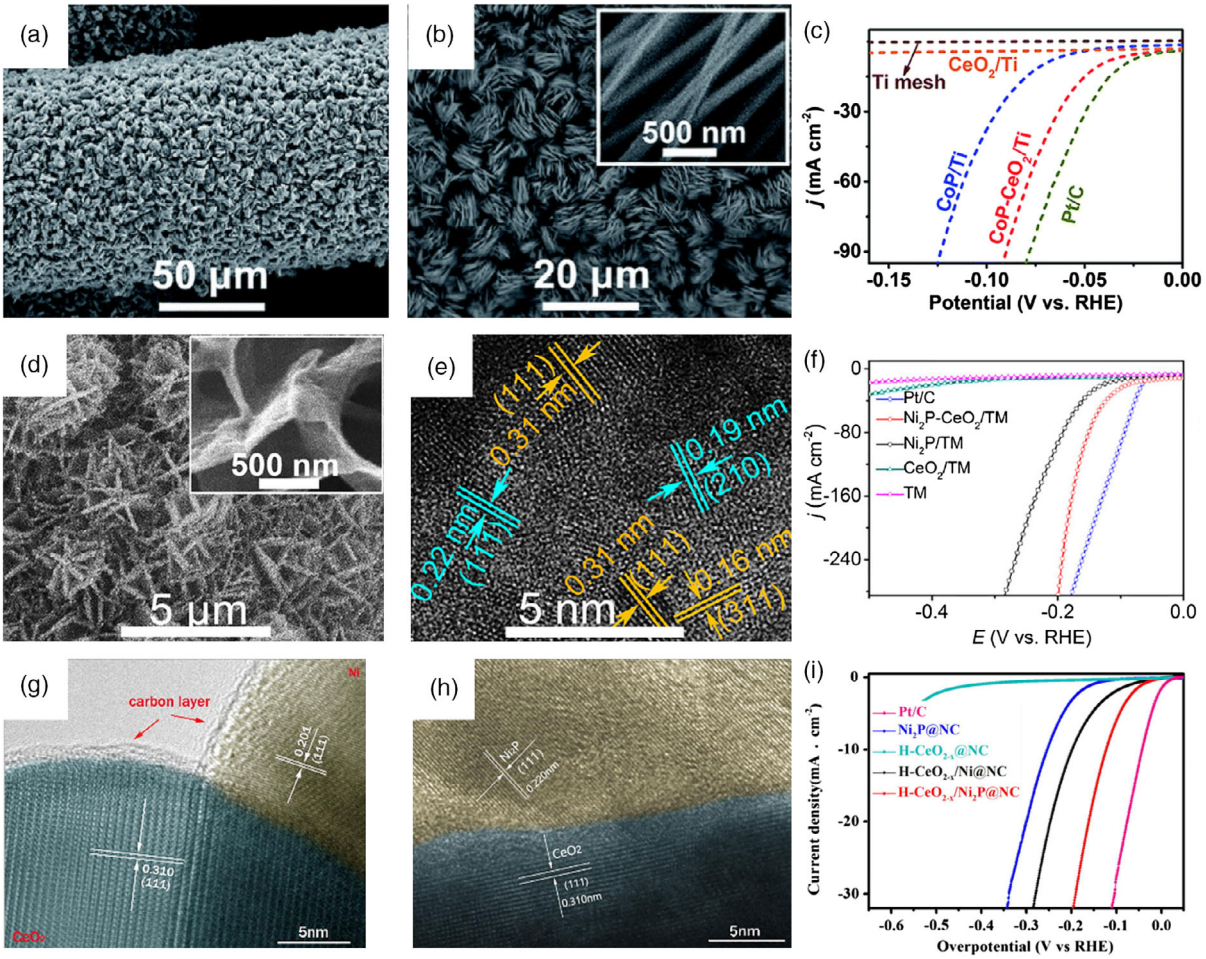

Figure 1. a,b) Scanning electron microscope (SEM) images of CoP–CeO_2/Ti and c) polarization curves of Ti mesh, CeO_2/Ti, CoP/Ti, CoP–CeO_2/Ti, and Pt/C on Ti mesh for the HER at a scan rate of 2 mV s^{-1} Reproduced with permission.[28] Copyright 2018, Royal Society of Chemistry. d,e) SEM and high-resolution transmission electron microscopy (HRTEM) images of NiP–CeO_2. f) Polarization curves for HER on Pt/C loaded on TM, Ni_2P–CeO_2/TM, Ni_2P/TM, CeO_2/TM, and bare TM. Reproduced with permission.[29] Copyright 2018, American Chemical Society. g,h) HRTEM images of H-CeO_{2-x}/Ni@NC and H-CeO_{2-x}/Ni_2P@NC. (i) Polarization curves of different catalysts tested in 1.0 M KOH. Reproduced with permission.[30] Copyright 2019, Elsevier.

© 2021 The Authors. Advanced Energy and Sustainability Research published by Wiley-VCH GmbH

Table 1. Summary of the HER catalytic property of various CeO_2-based electrocatalysts.

Electrocatalyst	Overpotential @10 mA cm^{-2} [mV]	Tafel slope [mV dec^{-1}]	Electrolyte	Ref.
3D–rGO–CeO_2	340	112.8	1 M KOH	[19]
Pd/CeO_2/C	109	75	1 M KOH	[21]
Ru^0/CeO_2	47	41	0.5 M H_2SO_4	[22]
Rh^0/CeO_2	42	34	0.5 M H_2SO_4	[23]
Ni–CeO_2/Ti mesh	67	111	1 M KOH	[24]
Co@CNT/CeO_2	181	90	1 M KOH	[25]
CeO_2–CoP–C	71	53	0.5 M H_2SO_4	[27]
CoP/CeO_2	43	45	1 M KOH	[28]
Ni_2P/CeO_2	84 [20 mA cm^{-2}]	113	1 M KOH	[29]
Ni–S/CeO_2	180	158	1 M NaOH	[31]
CeO_{2-x}/Ni_2P@NC	123	60	1 M KOH	[30]
Ni_3N–CeO_2	80	122	1 M KOH	[32]

catalysts for promoting HOR.[33] A peak power density of 1.4 W cm^{-2} was achieved due to the engineered Pd-to-CeO_2 interfacial contact. Furthermore, the DFT calculations suggest that the enhanced HOR activity is ascribed to a weakening of hydrogen binding energy through the interaction of Pd with the oxygen of CeO_2, which is facilitated by the structure of "oxidized Pd atom coordinated by four O atom on CeO_2." Similarly, the Pd/CeO_2 or Pd–CeO_2/C catalysts that were constructed by interface engineering,[34] surface doping,[35] entrapping,[36] depositing,[37] and so on show promoted activity for HOR.[38,39] Not only Pd-based electrocatalysts but also the oxygen-vacancy-rich CeO_2/Ni heterostructures were also synthesized to enhance HOR.[8] The thermoneutral adsorption free energies of H* caused by the electron transfer between CeO_2 and Ni combined with promoted OH* by abundant oxygen vacancies lead to an excellent HOR performance (0.038 mA cm_{Ni}^{-2} and 12.28 mA mg_{Ni}^{-1}). Furthermore, the Ir/CeO_2–C also displayed an enhanced activity due to the oxophilic effect caused by the higher oxygen storage–release capacity of CeO_2.[40] To summarize, CeO_2 is able to modulate the coordination environment of active components or sites to be more suitable for adsorbing H* and OH*, and so promote HOR.

2.3. Oxygen Evolution Reaction

As the other half-reaction of water splitting, OER is a four-electron transfer reaction, which is considered as the major bottleneck for water splitting because of the sluggish kinetics. Obviously, the OER is the key step to govern the overall efficiency of water splitting so that developing the highly active catalysts for OER is significant to improve the efficiency of water spitting. The conventional adsorbate evolution mechanism for HER is widely accepted and OH^- adsorbs on the surface oxygen vacancy site at the beginning.[41] Oxygen vacancy in the catalysts that has been reported can affect the surface charge distribution and further promote OER. Therefore, the CeO_2 in OER catalyst not only functions as a support but also mediates the surface charge distribution and regulates the adsorption/ desorption energy of reactants, products, and intermediates. Yang et al. prepared two morphologies of CeO_2 (nanowires and nanospheres) by the hydrothermal method and compared their OER activities. As a result, the nanospheres possess a stronger catalytic ability than nanowires due to the higher oxygen vacancy concentration in CeO_2 nanosphere.[42]

Considering the poor conductivity of CeO_2, the hybrid electrocatalyst has been synthesized with a combination of different materials. Recently, a CeO_2 decorated reduced graphene oxide was fabricated and it shows an enhanced HER activity, which results from the synergistic effect of oxygen vacancies on CeO_2 and electronic conductivity of reduced graphene oxide.[43] RuO_2 is one of the most active catalysts for OER, and researchers identified that the enhanced activity and stability in an alkaline solution of Ru^0/CeO_2 and RuO_2/CeO_2 catalysts was attributed to the highly oxidative oxygen species O_2^{2-}/O^- formed in the oxygen vacancy of CeO_2.[44,45] Transition metal-based catalysts are also reported as the low-cost and highly active catalyst solution for the OER, which have been widely studied as an alternative to replace the precious metal catalysts. CeO_2 decorated $Ni(OH)_2$ catalysts were fabricated and their catalytic performance for OER was studied (**Figure 2**a–e).[46,47] As a result, the introduction of CeO_2 nanoparticles not only creates more active species of $Ni^{3+/4+}$ but also accelerates the charge transfer efficiency, which significantly promotes the OER (Figure 2f,g). Wu et al. reported a Ni_3S_2–CeO_2 hybrid nanostructure by an electrodeposition method. The interfacial interaction between Ni_3S_2 and CeO_2 improves the electron transfer and enhances OER activity by increasing the binding strength of the reaction intermediates at the interface.[48] The bimetal alloy and hydroxide were also composited with CeO_2 to enhance the OER activity.[49–53] Chen et al. constructed Fe_xNi_y/CeO_2/NC catalyst and attributed its enhanced OER activity to the high oxygen-storage capacity of CeO_2, which enabled the immediate adsorption of the generated O_2 during OER process.[51] Transition metal oxide was considered as an important type of OER catalyst due to the remarkable redox capability and mixed valences. Therefore, transition metal oxide was fabricated as a special structure compositing with CeO_2 to promote OER. Hollow Co_3O_4/CeO_2 heterostructures embedded in N-doped carbon nanofibers were prepared by the electrospinning technique. The synergistic effects between Co_3O_4 and CeO_2 benefit the OER (Figure 2h–j).[43] More recently, Qiu et al. combined CeO_2 and Co_3O_4 by built-in pn heterojunction to promote OER.[54] The strongly coupled pn heterojunction interface leads to a rapid interfacial charge transfer from CeO_2 to Co_3O_4 and the resulting high concentration of oxygen vacancies and Co^{2+} octahedral sites enhances the OER activity. $FeCoO_4$/CeO_2 interface and 3D self-supporting porous network $NiCeO_x$@$NiFeO_x$ structure were also fabricated to enhance OER activity and the increased oxygen vacancy due to Ce^{3+}/Ce^{4+} was proved to promote the intrinsic OER activity of catalysts.[52,53] A quinary metal oxide $Ni_{0.3}Fe_{0.07}Co_{0.2}Ce_{0.43}O_x$ was prepared by Haber et al. to promote OER.[55] Subsequently, a similar (Ni–Fe–Co–Ce)O_x was prepared by Favaro et al. and studied under the operando conditions to expand the fundamental understanding of the active site. It turns out that the

© 2021 The Authors. Advanced Energy and Sustainability Research published by Wiley-VCH GmbH

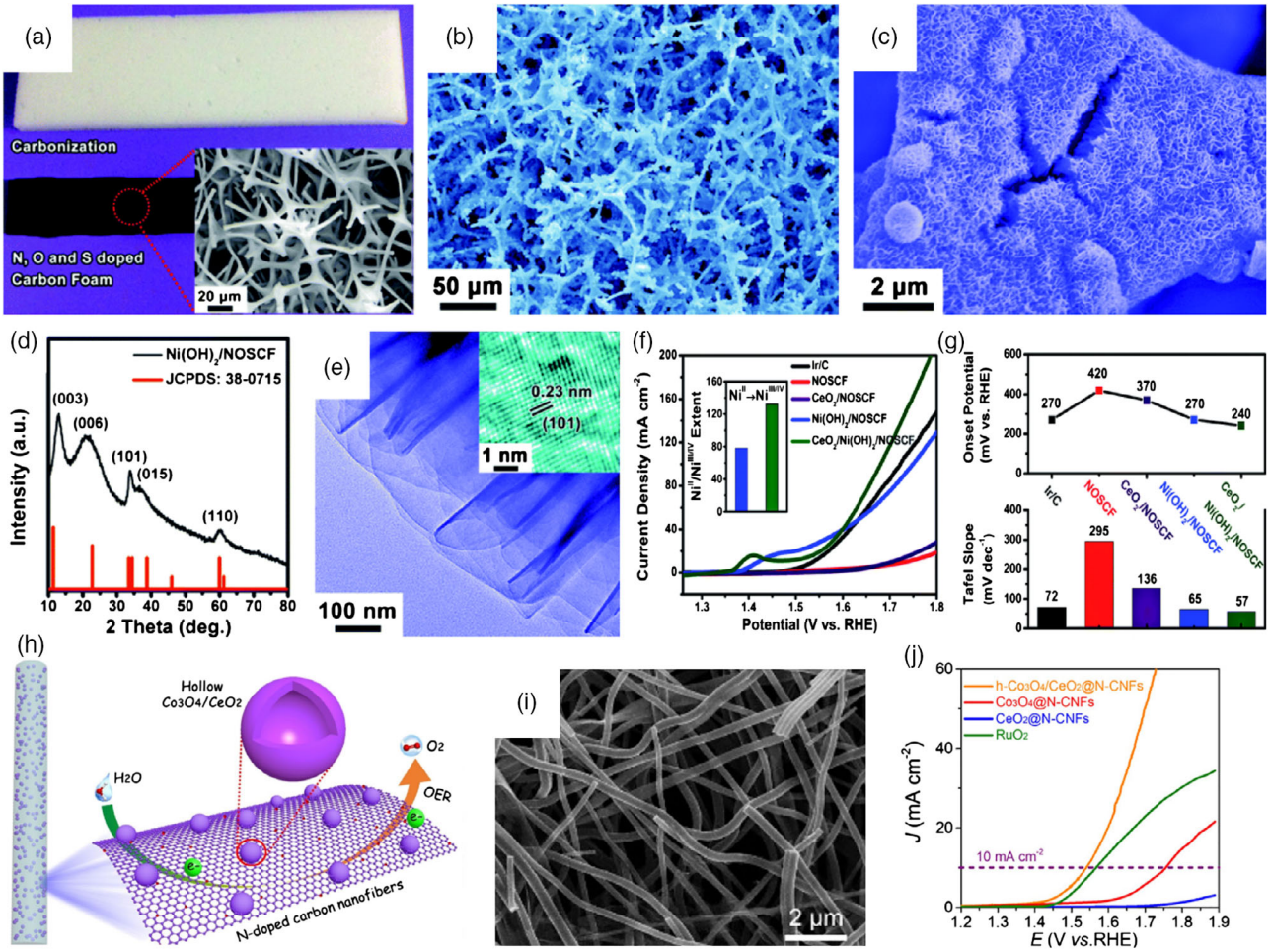

Figure 2. a) Carbon foam derived from a piece of melamine. b–d) SEM images and XRD pattern of $Ni(OH)_2$ nanosheets grown on NOSCF. e) HRTEM image of $Ni(OH)_2$ at the edge of the $Ni(OH)_2$/NOSCF. f) Polarization curves of different catalysts. g) The corresponding onset potential and Tafel curves for the catalysts derived from (f). Reproduced with permission.[46] Copyright 2017, Royal Society of Chemistry. (h) Schematic diagram of hollow Co_3O_4/CeO_2 embedded in N-doped carbon nanofibers. i) SEM of h-Co_3O_4/CeO_2@N–CNFs. Reproduced with permission.[43] 2019, American Chemical Society. j) Linear sweep voltammetry polarization curves of different catalysts in O_2-saturated 0.1 M KOH.

CeO_2 can affect the redox process of transition metals, which boosts the OER activity at low overpotential.[56] Furthermore, several Co-based catalysts like Co, CoO_x, CoP, $CoSe_2$, and $NiCo_2S_4$ were combined with CeO_2 to enhance OER activity.[57–61] CeO_2 not only enhances catalytic activity but also stabilizes the catalysts. Obata et al. coated CeO_x layer on $NiFeO_x$ to prevent the loss of Fe species during the OER process and achieved a highly stable performance.[62] The CeO_x layer does not affect the OER activity of $NiFeO_x$ because it selectively allows the permeation of OH^- and O_2 through but prevents the diffusion of redox ions through the layer. Conclusively, on the one hand, the oxygen vacancy on CeO_2 can promote the adsorption of OH^-, a step that occurs in OER. On the other hand, the oxygen vacancy often interacts with active components to produce special electronic structure that is conductive to the progress of OER, so, the rich oxygen vacancy in CeO_2 makes it a robust cocatalyst to enhance the catalytic activity of novel metal, transition metal, transition metal (hydro)oxides, transition metal phosphides, and bimetal alloy for OER (**Table 2**).

Based on the attractive catalytic performance for HER and OER of CeO_2-based catalysts, the related materials were also designed for overall water splitting. Tang et al. prepared hollow CeO_x/CoP heterostructures supported on nickel foam through co-based metal-organic frameworks template. The potential toward water splitting at 10 mA cm^{-2} was only 1.63 V and the catalyst performed excellent stability within 60 h.[63] Most recently, Du et al. synthesized superhydrophilic Co_4N–CeO_2 hybrid nanosheet array on a graphite plate for overall water splitting. The cell voltage to drive 10 mA cm^{-2} was 1.54 V and long-term durability at 500 mA cm^{-2} for 50 h. Doping CeO_2 into Co_4N not only promotes the dissociation of H_2O and adsorption of hydrogen but also improves the compositional stability, which boosting both OER and HER.[64] Therefore, CeO_2-based materials have great potential for water splitting, and more reasonable components and structures need to be explored and designed.

© 2021 The Authors. Advanced Energy and Sustainability Research published by Wiley-VCH GmbH

Table 2. Summary of the OER catalytic property of various CeO_2-based electrocatalysts.

Electrocatalyst	Overpotential @ 10 mA [cm^{-2} mV]	Tafel slop [mV dec^{-1}]	Electrolyte	Ref.
Ru^0/CeO_2	420	122.0	0.5 M KOH	[44]
$Ni(OH)_2/CeO_2$	320 [100 mA cm^{-2}]	126.0	1 M KOH	[47]
3D $CeO_2/Ni(OH)_2/C$	–	57.0	1 M KOH	[46]
$Fe_xNi_y/CeO_2/NC$	240	85.0	1 M KOH	[51]
$Ni_{90}Fe_{10}/CeO_2$	369	70.7	1 M KOH	[50]
NiFe–LDH/CeO_2@CeNC	235	128.8	1 M KOH	[49]
Co_3O_4/CeO_2	310	89.0	0.1 M KOH	[43]
$NiCeO_x$@$NiFeO_x$/Ni foam	254 [100 mA cm^{-2}]	59.9	1 M KOH	[52]
$FeCo_2O_4/CeO_2$	–	63.0	0.1 M KOH	[53]
V-CoP@CeO_2	225	58.0	1 M KOH	[57]
CeO_2/Co@NC	474	–	0.1 M KOH	[58]
CeO_x/CoO_x	331	66.0	1 M NaOH	[61]
$CeO_2/CoSe_2$	288	44.0	0.1 M KOH	[59]
$CeO_x/NiCo_2S_4$/CC	270	126	1 M KOH	[60]
Cu@CeO_2@Ni–Fe–Cr hydroxide	230.8	32.7	1 M KOH	[141]
CeO_x/NiFe–OH/Nickel foam	280 [100 mA cm^{-2}]	43.2	1 M KOH	[144]

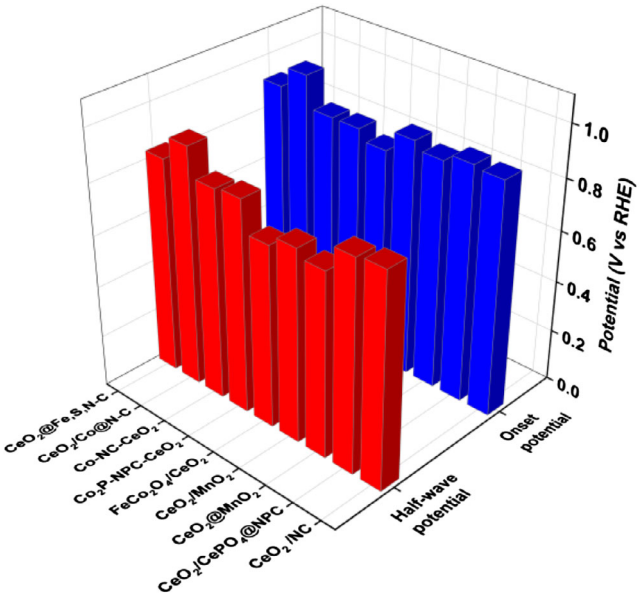

Figure 3. The onset potential and half-wave potential of CeO_2/NC[68], CeO_2/$CePO_4$@NPC,[80] CeO_2@MnO2,[75] CeO_2/MnO_2,[76] $FeCo_2O_4/CeO_2$,[53] Co_2P–NPC–CeO_2,[81] Co–NC–CeO_2,[77] CeO_2/Co@NC,[58] and CeO_2@Fe,S,N-C[82] for ORR.

2.4. Oxygen Reduction Reaction

Fuel cell is considered as one of the most promising energy-conversion devices due to its environmental friendliness, high efficiency, and reliability. Among them, the low-temperature PEMFCs attract wide attention due to their promising future in practical applications. However, the commercialization of PEMFCs has been limited by the sluggish ORR and the high cost of commercial catalyst Pt. Meanwhile, ORR is also an important cathodic half-reaction in rechargeable metal–air batteries and its slow kinetics severely restricts the power output. Although the Pt-based catalysts are state-of-art for ORR, the scarcity and high price of Pt promote us to develop low-cost and highly active catalysts. Recently, The CeO_2 nanomaterials and CeO_2 containing materials were designed to promote ORR in which the abundant oxygen vacancies on CeO_2 are able to regulate electronic structures of catalysts (**Figure 3**). Considering the poor conductivity of CeO_2, researchers combine the CeO_2 with functional carbon materials to enhance the conductivity of the composite catalysts. Peng et al. grew CeO_2 nanoparticles in situ on reduced graphene oxide (rGO) and found that the combinations of the high conductivity of rGO and sufficient active sites on CeO_2 enable the nanocomposite to become an efficient electrocatalyst for ORR.[65] Similar work has proved that the CeO_2/rGO nanocomposite is efficient not only for ORR but also for OER.[66] In addition to rGO, the C_3N_4 was chosen to composite with CeO_2 to enhance ORR catalytic activity since the pyridinic nitrogen in C_3N_4 functions as a promoter.[67] Most recently, Pi et al. fabricated CeO_2-encapsulated nitrogen-doped biochars for ORR in Zn/air batteries with remarkable performance.[68] Experiment combined with DFT illustrates that the Lewis base sites, produced by pyri-N and oxygen vacancy on CeO_2, remarkably promote the chemisorption of O_2 molecules. It is well known that Pt and Pd locate near the peak of the ORR volcano plot; however, the high expense and scarcity hinders the utilization in large-scale fuel cells.[69] Constructing the noble metal /CeO_2 catalyst can not only further enhance the catalytic activity and stability of the catalyst but also significantly reduce the loading of noble metal with improved utilization efficiency. Pinheiro et al. reported a hybrid electrocatalyst constructed by Pt nanoparticles and CeO_2 nanorods supported on carbon black for ORR with the aim of application in fuel cells.[70] As a result, the electrocatalyst shows an improved current and power density than the commercial Pt-based electrocatalysts. Li et al. obtained a similar result and attribute the enhanced performance to that the interaction between CeO_2 and Pt nanoparticles, which prevents surface Pt nanoparticles from aggregation.[71] Moreover, Du et al. consider that the CeO_2 modifies the electronic density of Pt, which enhances the interactions between Pt and C at the Pt–CeO_2 interface.[72] In addition, Pt and Pd were also used to fabricate the ORR electrocatalyst by combining CeO_2 and N-doped graphene.[73,74] Transition metal (oxides) is a kind of low-cost but high active electrocatalyst. Researchers have devoted efforts to build various nanostructures to improve their catalytic activity. A hierarchical CeO_2@MnO_2 core–shell composite and multiple hollow CeO_2 sphere decorated MnO_2 microflower were constructed by Yang et al. to catalyze ORR.[75–78] The enhanced catalytic performance was simply ascribed to the synergetic effect of CeO_2 and MnO_2. Also, porous hexagonal $FeCo_2O_4/CeO_2$ heterostructures were prepared. Depending on the abundant interfaces between $FeCo_2O_4$ and CeO_2, the high ORR catalytic activity is realized.[53] Doping strategy was considered as an efficient method to improve the performances of electrocatalysts. For both Co-doped

© 2021 The Authors. Advanced Energy and Sustainability Research published by Wiley-VCH GmbH

CeO_2 or Co-doped carbon, the ORR catalytic activities of catalysts are significantly improved.[77,78] Similarly, Sivanantham et al. constructed CeO_2 supported Co in N-doped carbon nanorods and ascribed the improved ORR activity to the synergistic effect of Co and coexistence of Ce^{3+} and Ce^{4+} in CeO_2.[79] Although Yu et al. considered the similar performance that originates from the synergistic effect between CeO_2 nanoparticles and N-doped carbon.[58] Furthermore, Co_2P and $CePO_4$ were also chosen to combine with CeO_2 and P, N co-doped carbon to make high performance catalysts for the ORR.[80–83] Therefore, CeO_2 not only possesses ORR active sites but also it can stabilize noble metals and improve the catalytic performance though electronic interactions. Moreover, the combination of CeO_2 and transition metal is an efficient alternative to develop low-cost and high activity ORR electrocatalysts.

2.5. Methanol/Ethanol Oxidation Reaction

Main direct alcohol fuel cells (DAFCs) have been considered as an attractive fuel device due to their volumetric energy density, environmentally friendliness, and abundant source of methanol or ethanol. The rate of M/EOR on the anode of DAFCs restricts the output power so that it is of great significance to develop efficient electrocatalysts for M/EOR. Similar to ORR, Pt is still the most effective electrocatalyst for M/EOR. However, compared to impressive progress in novel electrocatalysts for ORR, non-Pt catalysts seldom show the desired activity for M/EOR. For the application of Pt-based catalyst, suitable supports will have a key impact on the performance of catalysts and the utilization efficiency of Pt. The interface between active metal and support usually functions as the catalytic active sites due to the special

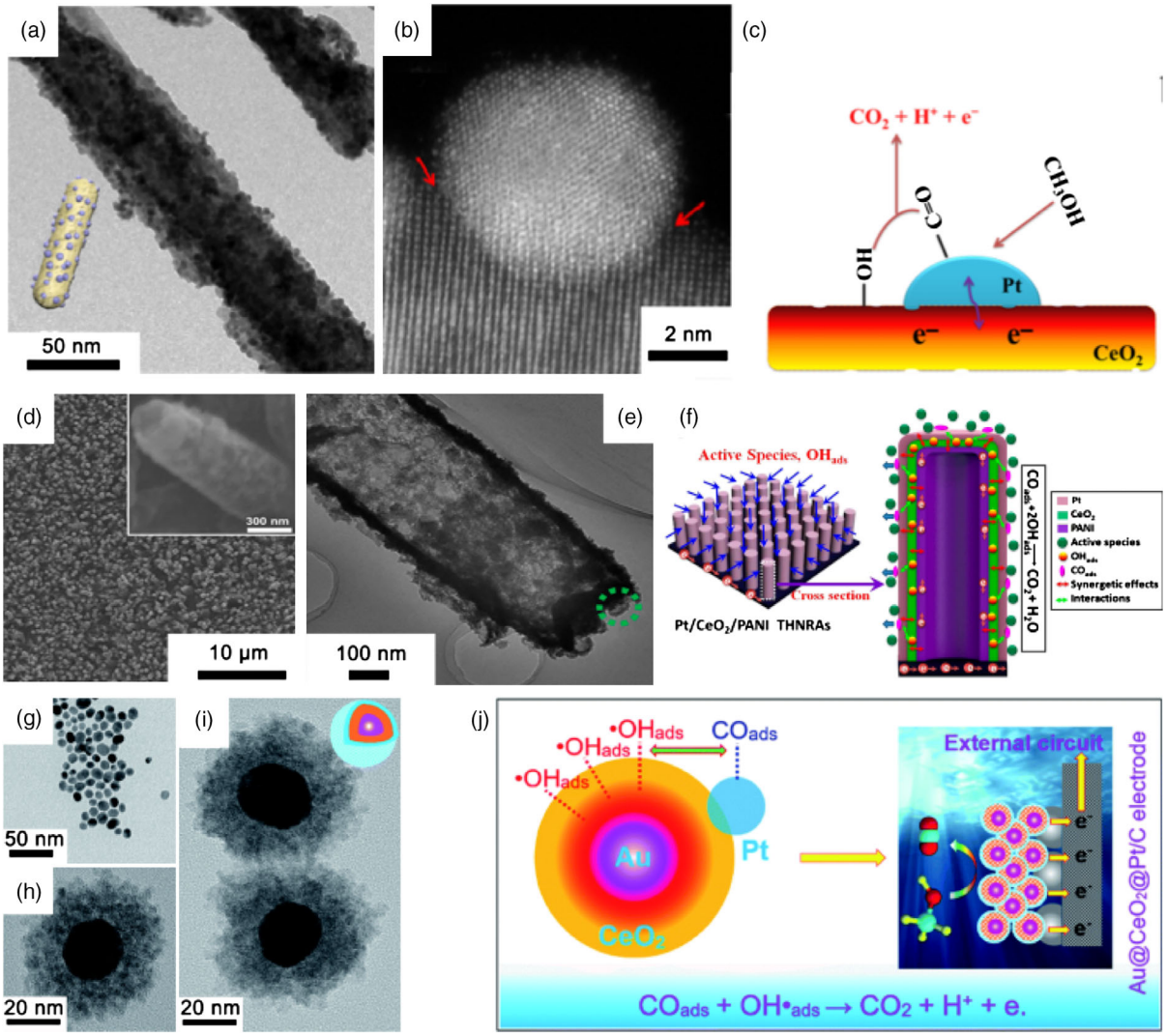

Figure 4. a,b) TEM and aberration-corrected high-angle annular dark-field scanning transmission electron microscopy (HAADF–STEM) images of Pt/CeO_2-P. c) The illustration graph of Pt on oxygen vacancy rich CeO_2. Reproduced with permission.[84] Copyright 2018, Elsevier. d,e) SEM and TEM image of Pt/CeO_2/PANI hollow nanorods arrays. f) Schematic diagram of Pt/CeO_2/PANI three-layered hollow nanorod arrays. Reproduced with permission.[90] Copyright 2016, American Chemical Society. g–i) The HRTEM of Au core, Au@CeO_2 core–shell and Au@CeO_2@Pt nanocatalyst. j) The plausible mechanism of the Au@CeO_2@Pt/C electrocatalyst toward methanol oxidation reaction. Reproduced with permission.[94] Copyright 2019, Royal Society of Chemistry.

© 2021 The Authors. Advanced Energy and Sustainability Research published by Wiley-VCH GmbH

lattice and electronic structure. Wang et al. constructed the interface between Pt nanoparticles and CeO_2 rods for MOR (**Figure 4**a,b).[84] They discovered that the oxygen vacancy on CeO_2 can supply electrons, which will increase the electron density of Pt by promoting the electron transfer from CeO_2 to Pt, and then, the enhanced catalytic activity and durability of Pt/CeO_2-rod are expected (Figure 4c). Chen et al. synthesized a Ce-modified Pt nanoparticle for MOR and high electrocatalytic activity was achieved (1470 mA mg_{Pt}^{-1} and 8670 mA mg_{Pt}^{-1} in acidic and alkaline media, respectively).[85] DFT calculations indicated that the modification of Ce deforms the Pt surface, which strengthens CO* + OH* bind. The stronger anchoring of OH* removed CO* more easily in the potential determining step, which avoids the CO-poisoning effect easily. Paulo et al. reported that catalytic performances of unsupported Pt nanoparticles for EOR in the acid medium are promoted by adding small amounts of CeO_2 nanoparticles.[86]

In addition to the influences on the electronic structures, CeO_2 nanoparticles are also able to generate microstrain on the surface Pt, which governs the electrochemical surface area for EOR. Obviously, the size and morphology of CeO_2 have a crucial effect on the catalytic properties of Pt/CeO_2 catalyst. Feng et al. prepared CeO_2 nanoparticles with well-defined morphologies (nanooctaherda, nanosphere, and nanocube) in which the Pt/CeO_2 nanosphere shows the highest catalytic activity for MOR.[87] Meanwhile, Chen et al. pointed out that the CeO_2 rod exposing (100)/(110) facets are responsible for the higher catalytic activity for MOR than CeO_2 plates and cubes in Pt/CeO_2 catalyst.[88] The higher Pt nanocrystals trapping ability and metal-support interaction were considered to be responsible for the enhanced performance of Pt/CeO_2 rod. More interestingly, there is also physical interaction between Pt and CeO_2, which allows Pt nanoparticles to highly disperse on CeO_2. Although CeO_2 performs well in Pt/CeO_2 catalysts, the poor conductivity still limits its application. To overcome this issue, researchers composite Pt/CeO_2 with highly conductive multiwalled carbon nanotube (MWCT),[89] rGO, and polyaniline[90,91] (Figure 4d–f). In addition, the modification of CeO_2 is also a strategy to develop highly efficient supported Pt-based catalysts. Xie et al. used the Cu-doped CeO_2 as a good support to fabricate Pt/C-$Ce_{0.8}Cu_{0.2}O_{2-\delta}$ catalyst and the introduction of Cu increases both the amount of oxygen vacancy and electric conductivity of CeO_2.[92] ZnO was also doped to Pt/CeO_2 nanofibers to promote surface reaction sites, reactive oxygen species, and the interactions between Pt and CeO_2 for MOR.[93] Dao et al. constructed Au@CeO_2 core–shell supported Pt catalyst for MOR (Figure 4g–i).[94] The catalyst showed not only a good catalytic activity but also high CO tolerance because that Au@CeO2 core–shell structure promotes the oxidation of CO (Figure 4j). In addition to modifying the support, alloying Pt with another transition metal is another efficient method to improve the catalytic performance for M/EOR.[95–97] Although CeO_2 is often used to construct Pt-based catalysts, the applications of it in non-Pt catalyst are also effective. Chai et al. prepare the Ir_3Sn–CeO_2/C catalyst for EOR and the catalyst was proved to be more active and stable than comparison Pt/C.[98] Most recently, NiO and rGO were used to composite with CeO_2 aiming at promoting MOR, and enhanced catalytic performance was achieved.[99,100] Therefore, the introduction of CeO_2 to electrocatalyst stabilizes the active metal to achieve the well dispersion as well as regulates the electronic of active metals. Since CeO_2 plays a key role in improving the catalytic performance of Pt-based catalysts, introducing CeO_2 into non-Pt catalyst with the aim of enhancing catalytic activity is worth doing.

2.6. CO_2 Reduction Reaction

Electroreduction of CO_2 is another important energy conversion reaction to generate liquid fuels and value-added chemicals. CO_2RR is a multielectron reaction involving different reaction intermediates and a vast number of possible final products (carbon monoxide, formate, formaldehyde, methane, methanol, methanol, and C_{2+} hydrocarbons and oxygenates). Due to the wide variety of reaction products, developing catalysts with high activity and selectivity is the most crucial task, which has attracted the intensive interest of researchers. The active metals of CO_2RR catalyst were classified according to their selectivity: carbon monoxide (Au, Ag, etc.), formate (Pb, Sn, etc.), hydrocarbons (Cu, etc.), and hydrogen (Pt, Ni, etc.). Researchers recently discovered that CeO_2 as an active component or support is beneficial to the CO_2 adsorption and activation. Valenti et al. combined CeO_2 nanoparticles with conductive MWCTs for direct electrocatalytic reduction of CO_2 to formic acid.[101] Nonstoichiometric $Ce^{4+/3+}O^{2-x}$ reduced sites were proved as essential for the selective CO_2RR. Gao et al. constructed Au–CeO_x interface to enhance CO_2RR (**Figure 5**a–c).[17] Experiment combined DFT calculations indicated that Au–CeO_x interface was the active site for CO_2 activation and reduction by promoting the stability of key carboxyl intermediate (*COOH) (Figure 5b,c). Similarly, Zhu et al. manipulated the interface of small-size Au and CeO_2 nanoparticles through adjusting the surface charge of Au and CeO_2, which leads to the utmost utilization of Au and enhancement of CO_2 adsorption.[102] Varandili et al. synthesized Cu/CeO_{2-x} nanocrystalline heterodimers by a colloidal seeded-growth technique for CO_2RR (Figure 5 d-g).[103] The Cu/CeO_{2-x} heterodimers exhibit high selectivity (≈80%) toward the CO_2RR against the competitive HER and a high Faradaic efficiency for methane (≈54%) (Figure 5 h). The catalytic performance was attributed to the formation of sufficient active sites at the interface, which strengthens the stabilization of intermediates CHO* through bidentate adsorption at Cu and oxygen vacancy on CeO_{2-x} site simultaneously. The interface effect not only promotes the CO_2RR but also strongly inhibits the competitive HER process. To further study the interaction between Cu and CeO_2 support, Wang et al. predicted through theoretical calculations that the single atomic Cu substitution in CeO_2 (110) surface generates three oxygen vacancies around Cu site, which are highly active catalytic sites for the initial CO_2 adsorption and subsequent activation.[18] Cu-doped mesoporous nanorods, which partially expose the (110) plane, were targetedly synthesized and its catalytic performance was consistent with the theoretical calculations.

Wu et al. reported CeO_2 doped with Cu^+ for CO_2RR and it shows the high faradaic efficiency for ethylene (47.6%) with long-term durability.[104] Furthermore, the methane selectivity is improved by comparing with 0D Cu. In this catalyst, CeO_2 function as the stabilizer for Cu^+. So, for Cu-based

© 2021 The Authors. Advanced Energy and Sustainability Research published by Wiley-VCH GmbH

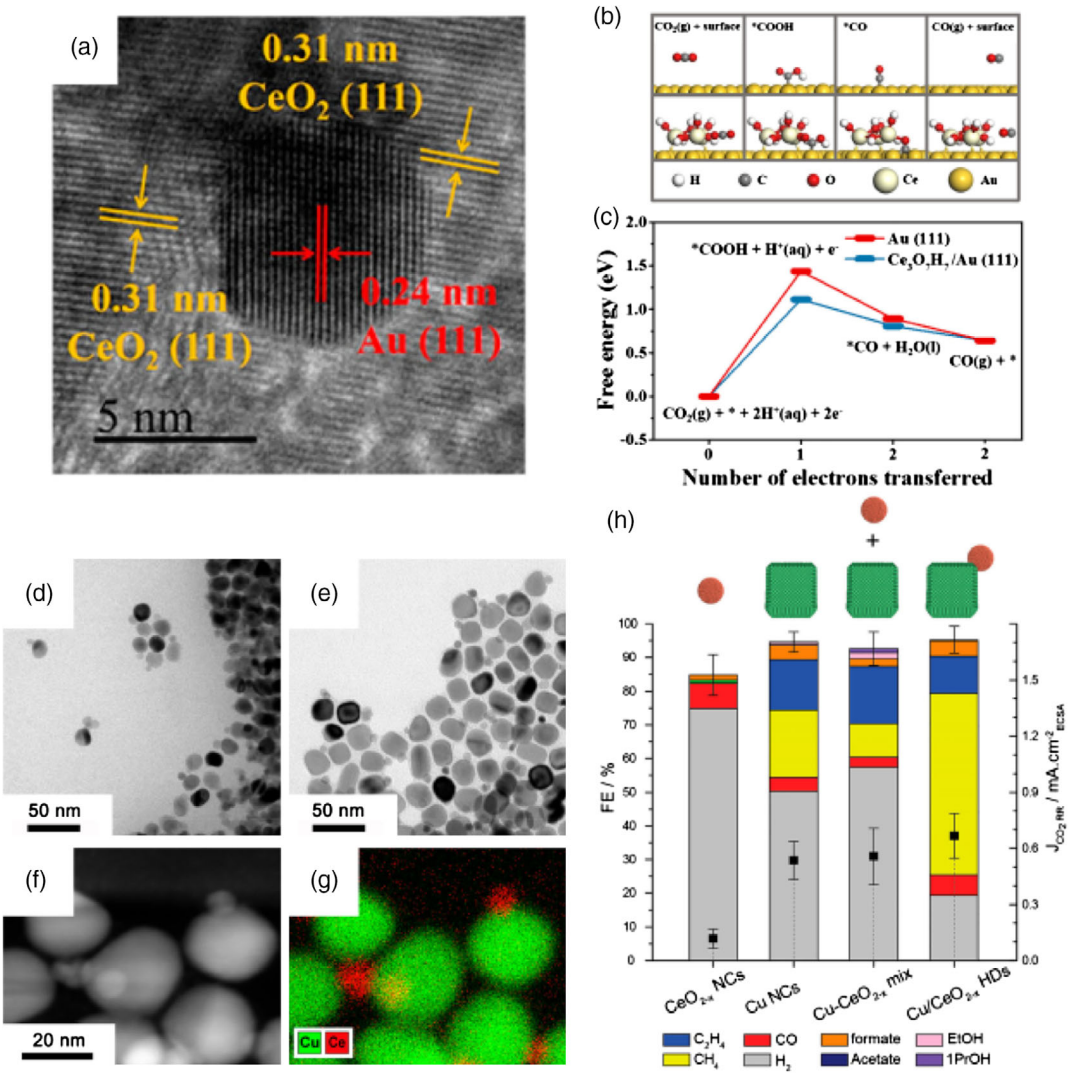

Figure 5. a) HRTEM image of Au–CeO_x/C catalyst. b,c) DFT calculation of CO_2RR at 0 V versus RHE on Au (111) surfaces. Reproduced with permission.[17] Copyright 2017, American Chemical Society. d,e) Bright-field TEM image of Cu/CeO_{2-x} heterodimers formed by injection of 0.1 and 0.2 mmol of CuOAc. f,g) HAADF–STEM image with the corresponding energy dispersive X-ray elemental maps of Cu and Ce in Cu (24 nm)/CeO2-*x* heterodimers. h) Faradaic efficiencies and CO_2RR partial current-densities for Cu/CeO_{2-x} heterodimers, Cu–CeO_{2-i} mix, Cu nanocrystals, and CeO_{2-i} nanocrystals. Reproduced with permission.[103] Copyright 2019, American Chemical Society.

electrocatalysts, the CeO_2 can not only enhance the activity but also improve the selectivity of methane. In addition to Cu, transition metal oxides are also used as active components of catalysts for CO_2RR. Zhang et al. constructed Co_3O_4–CeO_2/low graphitic carbon, which can efficiently reduce CO_2 to formate at only −0.31 V versus reversible hydrogen electrode (RHE).[105] They indicate that the oxygen vacancies enriched by the addition of Co_3O_4 are the key reason for the inhibited HER, enhanced activity, and stable formate selectivity. In summary, for electrocatalytic CO_2 reduction, CeO_2 not only enhances the activity but also has a certain impact on the selectivity of CO_2RR and it depends on the specific active components. Therefore, based on these results, CeO_2 is the ideal component to fabricate CO_2RR catalysts through the combination with other transition metal based materials.

2.7. N_2 Reduction Reaction

NH_3 is considered as one of the most important industrial chemicals and it is mainly synthesized from N_2 through harsh reaction conditions (Haber–Bosch process), which shows a tedious reaction process and high cost. Electroreduction of N_2 realizes the reaction in the facile environment. The N_2 reduction reaction (NRR) involves a six-electron transfer process and multiple intermediates due to the different reaction mechanisms. Similar to the CO_2RR, HER is also the main competing reaction, which makes selectivity a great challenge. CeO_2 itself is selected to be the catalysts for NRR. Xu et al. performed NRR on CeO_2 nanorods without any modification and discovered that CeO_2 with oxygen vacancy is catalytic active for NRR.[106] Meanwhile, Xie et al. also anchored ultrasmall CeO_2 on rGo to improve the

© 2021 The Authors. Advanced Energy and Sustainability Research published by Wiley-VCH GmbH

conductivity of CeO_2.[107] Many reports point that the electrocatalytic activity of the reported electrocatalyst is related to the abundant oxygen vacancies in CeO_2. Zhang et al. synthesized Cu-doped CeO_2 nanorods and found that Cu doping can effectively enrich the concentration of multiple oxygen vacancies, which significantly enhances NRR activity.[108] Similarly, Xie et al. prepared Cr-doped CeO_2 to increase the oxygen vacancies for NRR and an enhanced activity was achieved at −0.7 V versus RHE[109] Amorphous materials are more catalytically active to some degree because they usually exhibit "dangling bonds". CeO_x has been applied to induce the amorphization of Au nanoparticles on rGO by Li et al.[110] The amorphous Au shows strong structural distortion with more active sites for NRR, which shows higher ammonia yield (8.3 μg h^{-1} mg^{-1}_{cat}) and Faradaic efficiency (10.10%) at −0.2 V versus RHE than the crystalline counterpart. Similarly, Lv et al. prepared an amorphous $Bi_4V_2O_{11}$/CeO2 hybrid through a spinneret electrospinning method. The CeO_2 functions as a trigger to induce the amorphous phase and promotes the interfacial charge transfer by build band alignment with $Bi_4V_2O_{11}$.[111] In addition, CeO_2 supported single metal atoms become potential electrocatalysts for NRR. To prove it, Qi et al. conducted DFT calculations on transition metal atomic catalysts supported by stepped CeO_2.[112] The screening results showed that Nb, V, Ru, Mo, W, and Os atoms supported on CeO_2 are possible NRR catalysts. Therefore, both experimental and theoretical calculations indicate that CeO_2 plays a key role to enhance the catalytic activity for NRR, and CeO_2-based NRR catalyst deserves more attention in the future due to their potential.

3. CeO_2-Based Photocatalyst

3.1. Hydrogen Evolution Reaction

In addition to the electrically driven water splitting reaction, the photocatalytic HER is another promising approach to produce H_2 by an environment-friendly way. Semiconductor photocatalysis for efficient water splitting has attracted lots of research in which the narrow bandgap and imperative photoredox behavior are fundamental required properties. Because of the easy conversion between Ce^{3+} and Ce^{4+} and rich oxygen vacancies, nanostructured CeO_2 often was used as support or composite material to enhance photocatalytic activity.[113,114] Dong et al. prepared CeO_2 nanorods and found that the bare CeO_2 without compositing any other active component shows photocatalytic activity.[115] The H_2 production rate of 5.02 μmol g^{-1} h^{-1} under solar light irradiation was achieved, and the photocatalytic activity was related to the conversion of Ce^{3+}/Ce^{4+} and oxygen vacancies. Krishnan et al. reduced the bandgap of CeO_2 to 2.5 by adding Fe_2O_3, which endows CeO_2 absorption in the visible region, enhanced charge separation, and low rate of electron–hole pair recombination.[116] CdS is an extensively studied photocatalyst due to its appropriate bandgap (≈2.4 eV) and superior sensitizing properties. Compositing CdS with CeO_2 is an approach to further improve the photocatalytic activity. Zheng et al. fabricated ultrathin CdS shell-sensitized S-doped CeO_2 hollow spheres, which exhibits remarkably enhanced photocatalytic activity for HER (1147.2 μmolg^{-1} h^{-1}) under visible light illumination (**Figure 6**a,b).[117] The oxygen vacancies in S-doped CeO_2 reduced bandgap of catalysts and the CdS sensitization effect promotes the interface carrier separation and transfer, which results in superior photocatalytic performance (Figure 6c). CdS quantum dot (QD) is a promising material for photocatalyst due to its unique small size (<10 nm), short effective charge transfer length, suitable bandgap, and extensive light-harvesting. Ma et al. constructed 0D/1D CdS QDs/CeO_2 nanorod heterojunction and noted the enhanced photocatalytic performance.[118] The 0D/1D CdS QDs/CeO_2 heterojunctions provide stronger electronic conductivity, improved light-harvesting, and enhanced photoresponse, which was beneficial for photocatalysts. Z-scheme heterojunction was widely studied because it enhances the separation efficiency of photogenerated electron–hole pairs and the reduction capacity of electrons participating in HER. The Z-scheme between CdS QDs and CeO_2 nanorods was a key factor in the increased photocatalytic performance. Moreover, Sultana synthesized ternary nanoheterostructure, CeO_2 nanosheets supported CdSQDs and Au nanoparticles.[119] The Au nanoparticle incorporated into the interface between CeO_2 and CdS QDs is a mediator, which injects hot electrons through the LSPR (light-induced surface plasmon resonance) effect, which is responsible for the enhancement in photocatalytic performance. Compared with CeO_2 supported QDs materials, CeO_2 QD embedded in porous carbon nanotubes (CNTs) by a versatile biotemplate method is also achieved.[120] In addition, Qian et al. synthesized in situ CeO_2–CuO QDs heterojunction on graphene and the p-type CuO/n-type CeO_2 heterojunction show a superior photocatalytic performance (H_2 evolution rate, 2481 μmolg^{-1} h^{-1}).[121] The pn heterojunctions in semiconductor-based photocatalysts is essential in promoting H_2 production. Swain et al. constructed p-MoS_2/n-CeO_2 heterojunction toward solar hydrogen production.[122] They found that the pn heterojunction provides an internal electric field to promote the photogenerated charge separation and transfer. A quaternary Cu_2ZnSnS_4 nanoparticle decorated CeO_2 pn heterojunction was reported by Sridharan et al., which reaches hydrogen production efficiency of 2930 μmolg^{-1} h^{-1}.[123] CeO_2 coupled Cu_2ZnSnS_4 induces the visible light absorption and separation, the transmission of photoinduced charge carriers, as well as impedes the rapid electron–hole pair recombinations. Wang et al. designed 0D/2D $Mn_{0.2}Cd_{0.8}S/CeO_2$ directed Z-scheme and photocatalytic H_2 production rate of 8.73 mmolg^{-1} h^{-1} was obtained in Na_2S/Na_2SO_3 aqueous solution.[124] $CeO_2/CeVO_4/V_2O_5$ was prepared to induce Z-scheme-charge-transfer and drive photocatalytic degradation coupled with H_2 generation.[125] The $CeVO_4$ nanoparticles function as a conductive channel to transfer photogenerated carriers, as redox centers to facilitate the transfer of photogenerated electrons and enhance the separation efficiency of electron–hole pair. Graphitic carbon nitride (g-C_3N_4) was considered as a promising candidate material for photocatalyst due to its medium bandgap (≈2.7 eV) and excellent photocatalytic stability. A new strategy that combines g-C_3N_4 with CeO_2 has been constructed for efficient water splitting. Liu et al. prepared g-C_3N_4 supported CeO_2 nanocomposites for photocatalytic HER and the hydrogen generation rate is 0.83 mmolg^{-1} h^{-1} under visible light illumination, which was ascribed to the interfacial effects caused more visible light absorbance and enhanced electron transfer.[126] Waqas et al. fabricated N-bonded CeO_{2-x}/g-C_3N_4 hollow structure

© 2021 The Authors. Advanced Energy and Sustainability Research published by Wiley-VCH GmbH

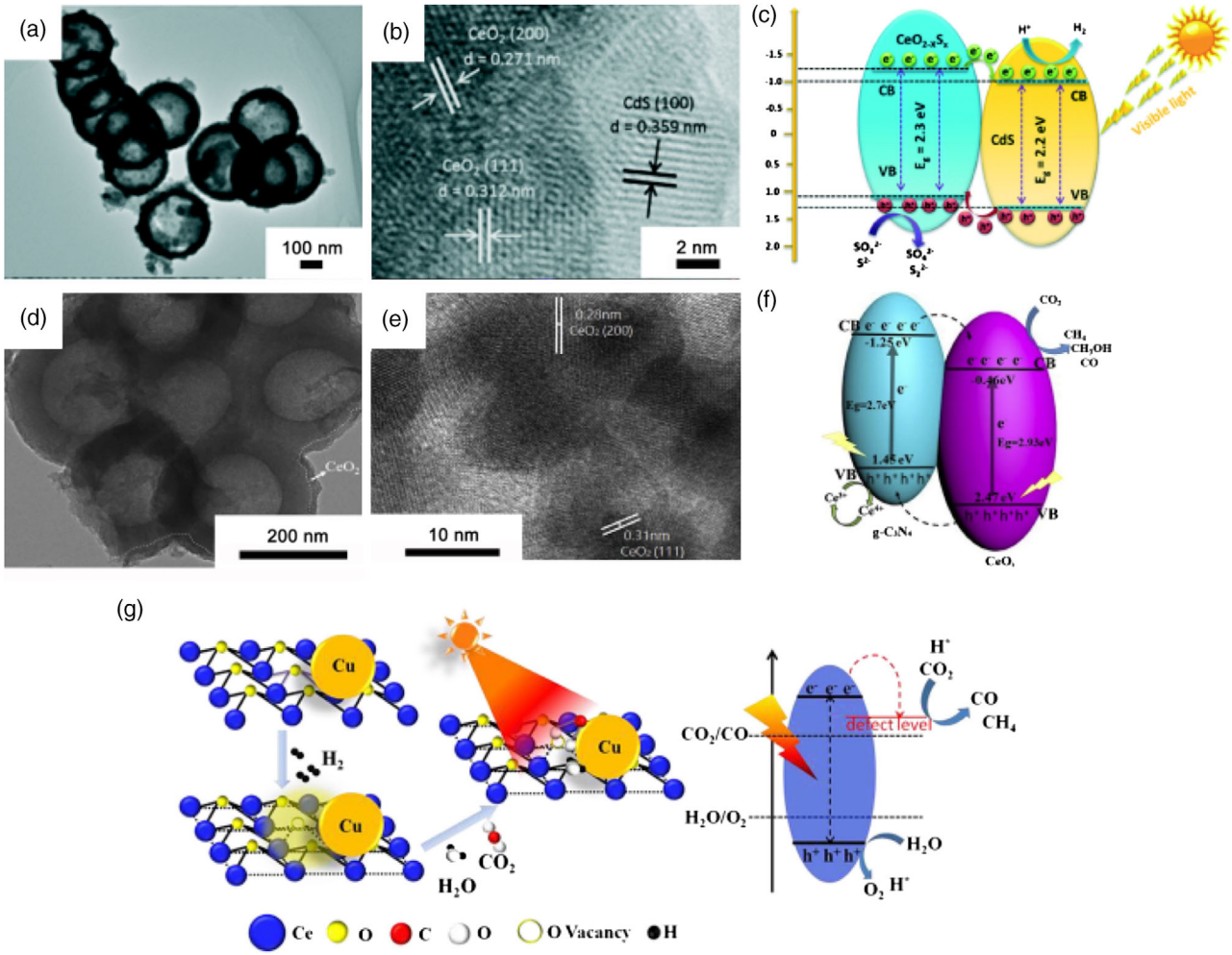

Figure 6. a,b) TEM and HRTEM images of $CeO_{2-x}S_x$@CdS composite. c) Schematic diagram of the proposed charge carrier transfer and H_2 evolution mechanism over the $CeO_{2-x}S_x$@CdS photocatalyst under visible light irradiation. Reproduced with permission.[117] Copyright 2019, Royal Society of Chemistry. d,e) TEM and HRTEM images of g-C_3N_4@CeO_2. f) Schematic illustration of band structure diagram and photoinduced carriers transfer of g-C_3N_4@CeO_2 under visible light irradiation. Reproduced with permission.[132] Copyright 2019, Elsevier. g) Scheme of possible mechanism of CO2 reduction on Cu/CeO_{2-x}. Reproduced with permission.[133] Copyright 2019, American Chemical Society.

by incorporating cyanamide molecules.[127] In this photocatalyst, hollow structure enhanced light-harvesting ability; Ce^{3+} functioned as optically active sites; inorganic/organic interfaces boosted the separation efficient of minority carrier. To further improve the photocatalytic activity for the water splitting, a ternary composite, CeO_2 nanocrystal-modified layered MoS_2/g-C_3N_4 was constructed.[128] The well-matched energy-level position and efficient charge separation caused by electron transfer processes between Ce^{4+}/Ce^{3+} pairs and heterostructures were responsible for the superior. Moreover, the interfacial electronic interaction and Ce^{3+} species promotes adsorption capacity and decreases energy barrier for reactant H_2O adsorption, which is beneficial for the water splitting. Similarly, CeO_2@Ni_4S_3/g-C_3N_4 synthesized by Yu et al. exhibits an enhanced photocatalytic activity under the visible light.[129] Therefore, the CeO_2 supported QDs materials, constructed pn heterojunction, and the Z-Scheme, etc. have exhibited superior photocatalytic performance due to the improved light harvesting, enhanced charge separation, and impeding the rapid electron–hole pair recombination. In conclusion,CeO_2 can not only play the role of active sites for photocatalytic HER but also more importantly, it can regulate the bandgap, enhance light harvesting, and impede the rapid electron–hole pair recombination of catalysts, which closely related to photocatalytic HER activity (**Table 3**).

3.2. CO_2 Reduction Reaction

Recently, photocatalytic CO_2RR has caught the researchers' eyes because it can produce value-added chemicals and energy-rich fuel while mitigating CO_2 emission. Many strategies have been applied to fabricate nanomaterials for CO_2RR, and compositing CeO_2 with traditional photocatalytic material is an effective method to promote CO_2 conversion.[101] Li et al. designed and synthesized mesostructured CeO_2/g-C_3N_4 to promote CO_2 photoreduction and the main product is CO and CH_4.[130] The

© 2021 The Authors. Advanced Energy and Sustainability Research published by Wiley-VCH GmbH

Table 3. Summary of the HER catalytic property of various CeO_2-based photocatalysts.

Photocatalyst	H_2 evolution rate [μmol h^{-1} g^{-1}]	Ref.
CdS QDs/CeO_2	101	[118]
Pt/CeO_2	19 700	[113]
CeO_2 QDs/C	582	[120]
Cu_2ZnSnS_4/CeO_2	2930	[123]
N-CeO_{2-x}/g-C_3N_4	43	[127]
$CeO_{2-x}S_x$@CdS	1147	[117]
$Mn_{0.2}Cd_{0.8}S$/CeO_2	8730	[124]
CeO_2–CuO QDs/graphene	2481	[121]
CeO_2–Au–CdS QDs	12 475	[119]
CeO_2	5	[115]
CeO_2/g-C_3N_4	830	[126]
CeO_2@Ni_4S_3/g-C_3N_4	3740	[129]
CeO_2–Fe_2O_3	584 [μmol h^{-1}]	[116]
p-MoS_2/n-CeO_2	721 [μA cm^{-2}]	[122]

enhanced photocatalytic performance is ascribed to the synergetic effect of mutual activations in CeO_2 and g-C_3N_4. Han et al. prepared a series of CeO_2-modified C_3N_4 and their band structures have been carefully revealed by both theoretical calculations and experimental characterizations.[131] It is noted that the CeO_2-modified C_3N_4 matches the energy, enhances the absorption in the visible region, and promotes the separation of photogenerated electron–hole pair, which improves the photocatalytic performance. Liang et al. synthesized the g-C_3N_4@CeO_2 photocatalyst with hollow heterostructures and rich oxygen vacancies. CO_2 has been selectively converted to CH_4, CH_3OH, and CO (Figure 6d–f).[132] The oxygen vacancies can facilitate charge separation and transfer. Meanwhile, the hollow frame improves the light efficiency due to the multiple reflections in the chamber. Wang et al. enriched and stabilized oxygen vacancies on CeO_2 by introducing Cu and as expected, the Cu/CeO_{2-x} showed the enhanced photocatalytic activity for CO yield.[133] The oxygen vacancies not only promote the separation and transfer of photogenerated charge carriers but also enhance the visible light absorption (Figure 6 g). Ag is a catalytically active metal for CO_2 reduction whether in electrocatalysis or photocatalysis. Wang et al. synthesized order mesoporous CeO_2 and constructed g-C_3N_4/Ag/CeO_2 composite. The ordered mesostructure is a merit for the CO_2 adsorption and migrations, where the g-C_3N_4 nanosheets can protect the Ag nanoparticles from photocorrosion to further boost the CO_2 photoreduction.[134] TiO_2 possesses many advantages such as high stability, nontoxicity, and low cost as a photocatalyst. Seeharaj et al. fabricated TiO_2/rGo/CeO_2 heterojunction with a modified surface to convert CO_2 to CH_3OH and C_2H_5OH.[135] The strong connection and high interfacial contact area between TiO_2 nanosheets, rGO, and CeO_2 promote the photogenerated charge carriers to react with adsorbed species, and the heterojunction effectively hindered electron–hole recombination. The rod-like attapulgite was used to modify spindle-structured CeO_2 to enhance photocatalytic performance for the CO_2 reduction.[136] The accumulation of CeO_2 was inhibited by the introduction of attapulgite and thereby the active sites for CO_2 conversion were increased. Moreover, a ternary photocatalyst consists of In_2O_3, CeO_2, and HCl treated attapulgite also present high activity for CO and CH_4 yields.[137] Doping is also an effective approach to enhance the photocatalytic activity of CeO_2 by extending the spectral response range and improving electronic conductivity.[138] In summary, oxygen vacancies not only promote the separation and transfer of photogenerated charge carriers but also enhance visible light absorptions. Therefore, abundant oxygen vacancies on CeO_2 and the formed heterostructure with other traditional photocatalytic materials results in the CeO_2-based photocatalyst high efficiency for CO_2 conversion.

4. Theoretical Explorations of CeO_2-Based Catalysts

In recent years, the significant contribution of CeO_2 in catalysis has been proved by many experiments. In the meantime, the theoretical calculations have also been applied in these electrocatalysts to supply more insights into improved performance. The intrinsic electroactivity of CeO_2 and the contribution to the electrocatalysis as catalyst support have been revealed by theoretical calculations in recent years.

The flexible switching between Ce^{3+} and Ce^{4+} due to the formation of oxygen vacancy formation is usually considered as the key reason for the high intrinsic electroactivity. In previous works, Huang et al. have studied the native defect formation in CeO_2 based on the DFTwith repulsive potential (DFT + U) method.[139] To reduce the calculation error induced by overlaps of valence-core charge density, they have selected the nonlinear core correction (NLCC) method for 4f levels in lanthanides. They have confirmed the low energy barrier of 0.39 eV for the formation of an oxygen vacancy. The identified negative U of oxygen vacancy further supports the excellent photocatalytic performance. Later in another work by Zhu et al, the high mobility of Ce with the formation of CeO_2 nanoclusters has been identified by the atomic-resolution electron energy-loss spectroscopic mapping.[140] The oxygen-exchange mechanism further supports the ability of mobile Ce^{4+} to carry oxygen or create oxygen vacancies to enhance oxygen transport. These preliminary works have supplied insightful information on the intrinsic activity of CeO_2. On the other side, CeO_2 plays a different role in catalysts for different material systems. In our previous works, we have successfully constructed the CeO_2-based composite electrocatalysts for OER.[141] Within such an interfacial structure, CeO_2 supplies the abundant 4f orbitals in a wide range as the "electron transfer expressway" to facilitate the electron transfer based on the d–f couplings between CeO_2 and NiFeLDH. This electronic environment is highly beneficial for high-speed charge transfer to promote the OER. Meanwhile, CeO_2 also plays as a good atomic catalyst support for Rh single atomic catalyst.[142] CeO_2 shows a good coupling effect with the anchoring Rh atoms to stabilize the surface atom, which also further optimizes the binding strength of CH_4 to achieve the oxidation process. In recent years, the theoretical investigation of CeO_2 is usually based on the transition

© 2021 The Authors. Advanced Energy and Sustainability Research published by Wiley-VCH GmbH

metal modification. For example, Wang et al. have reported the formation of oxygen vacancies in Fe, Co, and Ni-doped CeO_2 as well as their electroactivity for CH_4 activation.[143] They have systematically revealed the oxygen vacancy formation in (111) and (110) surfaces of the doped-CeO_2 surfaces. They also compared the CH_4 adsorption and C–H dissociation process based on the activation energy barriers. They concluded that the formation of oxygen vacancies is facilitated by the substitution of transition metals in the CeO_2, which is more energetically preferred than the adsorption and insertions of transition metals.

Although explorations on the CeO_2-based catalysts have been reported, the in-depth discussions from theoretical perspectives, especially for the photocatalytic performance, are still lacking. This is attributed to the challenge of accurate calculation in electronic structures of rare earth metal materials. Meanwhile, different combinations between CeO_2 and other material systems also supply significant references to the understanding of catalytic mechanisms. In the future, more efforts in the theoretical investigations of CeO_2-based catalysts are still highly needed.

5. Conclusion, Opportunities, and Outlook

This review systematically summarizes the application of CeO_2-based materials in the electrocatalytic and photocatalytic energy conversion-related reactions (HER, OER, ORR, M/EOR, CO_2RR, and NRR). CeO_2 was extensively used to composite with other catalytically active components to construct the special structure with enhanced electro(photo)catalytic performance. CeO_2 mainly disperse and anchor active component nanoparticles to increase the number of active sites, which demonstrates a strong electronic interaction with active components to achieve the regulation of their electronic structures, aiming to improve the intrinsic activity. The two important features of CeO_2, abundant oxygen vacancies and flexible transitions between Ce^{3+} and Ce^{4+}, play a key role to improve the electro(photo)catalytic activity of catalysts. Furthermore, we discussed the role of CeO_2 in different electro(photo)catalysts in detail. The activity and stability of different catalysts including novel metal, transition metals, transition metal phosphides, and transition metal nitrides catalysts are enhanced by compositing CeO_2 since it tends to regulate and optimize the electronic structure of the catalyst. The optimized reactant, intermediate, and product adsorption/desorption energy caused by modulating the electronic structure of catalysts leads to a promoted electrocatalytic performance. CeO_2 can not only play the role of active sites for photocatalysts but also more importantly, it can regulate the bandgap, enhance light harvesting, and impede the rapid electron–hole pair recombination of catalysts, which is closely related to the photocatalytic activity. However, there are still several challenges in the understanding and commercial application of CeO_2-based electro(photo)catalysts.

Therefore, to further rationally design and develop more efficient CeO_2-based electro(photo)catalysts with better performance, we believe the following aspects should be focused on: 1) further study the effect of oxygen vacancy and Ce^{3+}/Ce^{4+} ratio on catalytic activity combining theoretical calculations and in situ technologies. Most of the current works only qualitatively reveal that oxygen vacancy and Ce^{3+} are beneficial to catalytic activity, the direct evidence by advanced in situ technology, and theoretical calculations are still needed. A more accurate and in-depth understanding of this structure-activity relationship is of great significance for researchers to design and fabricate highly effective electro(photo)catalysts; 2) precise synthesis of CeO_2 with a controlled amount of oxygen vacancies and the ratio of Ce^{3+}/Ce^{4+}. Precise synthesis is the goal pursued in the field of material synthesis. It is not only vital to enhance catalytic performance but also to provide valuable references for our research on catalytic mechanisms; 3) based on the understanding of the effect of structure on catalytic performance, efficiently synthesized CeO_2-based materials with the specific structure are critical to the catalytic reaction. We should aim to conversely design and build specific nanostructures like hydrophilic/hydrophobic surface, array, core–shell, porous, and hollow structures, etc. to create more active sites and enhance the mass transfer for specific reactions; and 4) improve the conductivity of CeO_2-based materials to promote the transfer of electrons in the reaction by doping strategies, compositing highly conductive materials, and directly growing active materials on the conductive substrates (carbon cloth, metal foam, etc.).

In summary, although CeO_2-based catalysts have shown good performances in electro(photo)catalysis, there is still untapped potential for the improvement of properties and commercial applications. With the continuous efforts devoted by researchers and engineers, we believe that CeO_2-based catalysts will activate and convert energy-related small molecules more efficiently and be applied in industrial productions in the future.

Acknowledgements

The authors gratefully acknowledge the support from the China National Funds for Excellent Young Scientists (Grant No.: 21522106) and National Natural Science Foundation of China (Grant No.:21971117; 21771156), 111 Project (B18030) from China, and the Open Funds (RERU2019001) of the State Key Laboratory of Rare Earth Resource Utilization, the Functional Research Funds for the Central Universities, Nankai University (ZB19500202), the Shenzhen Fundamental Research Project (Grant No.: JCYJ20170818100717134), and the Early Career Scheme (ECS) fund (Grant No.: PolyU 253026/16P) from the Research Grant Council (RGC) in Hong Kong.

Conflict of Interest

The authors declare no conflict of interest.

Keywords

CeO_2-based materials, electrocatalysts, electronic interaction, oxygen vacancy, photocatalysts

Received: November 2, 2020
Revised: November 28, 2020
Published online: January 8, 2021

[1] S. Chu, A. Majumdar, *Nature* **2012**, *488*, 294.
[2] Z. W. Seh, J. Kibsgaard, C. F. Dickens, I. Chorkendorff, J. K. Norskov, T. F. Jaramillo, *Science* **2017**, *355*.

© 2021 The Authors. Advanced Energy and Sustainability Research published by Wiley-VCH GmbH

[3] M. B. Ross, P. De Luna, Y. Li, C.-T. Dinh, D. Kim, P. Yang, E. H. Sargent, *Nat. Catal.* **2019**, *2*, 648.
[4] I. Roger, M. A. Shipman, M. D. Symes, *Nat. Rev. Chem.* **2017**, *1*.
[5] M. K. Debe, *Nature* **2012**, *486*, 43.
[6] D. R. MacFarlane, P. V. Cherepanov, J. Choi, B. H. R. Suryanto, R. Y. Hodgetts, J. M. Bakker, F. M. Ferrero Vallana, A. N. Simonov, *Joule* **2020**, *4*, 1186.
[7] G. Zhao, K. Rui, S. X. Dou, W. Sun, *Adv. Funct. Mater.* **2018**, *28*, 1803291.
[8] F. Yang, X. Bao, P. Li, X. Wang, G. Cheng, S. Chen, W. Luo, *Angew. Chem. Int. Ed.* **2019**, *58*, 14179.
[9] J. Stacy, Y. N. Regmi, B. Leonard, M. Fan, *Renew. Sustain. Energy Rev.* **2017**, *69*, 401.
[10] L. Huang, X. Zhang, Q. Wang, Y. Han, Y. Fang, S. Dong, *J. Am. Chem. Soc.* **2018**, *140*, 1142.
[11] Y. Wan, J. Xu, R. Lv, *Mater. Today* **2019**, *27*, 69.
[12] J. Wang, X. Xiao, Y. Liu, K. Pan, H. Pang, S. Wei, *J. Mater. Chem. A*, **2019**, *7*, 17675.
[13] S. Xie, Z. Wang, F. Cheng, P. Zhang, W. Mai, Y. Tong, *Nano Energy* **2017**, *34*, 313.
[14] G. Lu, H. Zheng, J. Lv, G. Wang, X. Huang, *J. Power Source* **2020**, *480*, 229091.
[15] W. Gao, D. Wen, J.C. Ho, Y. Qu, *Mater. Today Chem.* **2019**, *12*, 266.
[16] M. Melchionna, P. Fornasiero, *Mater. Today* **2014**, *17*, 349.
[17] D. Gao, Y. Zhang, Z. Zhou, F. Cai, X. Zhao, W. Huang, Y. Li, J. Zhu, P. Liu, F. Yang, G. Wang, X. Bao, *J. Am. Chem. Soc.* **2017**, *139*, 5652.
[18] Y. Wang, Z. Chen, P. Han, Y. Du, Z. Gu, X. Xu, G. Zheng, *ACS Catal.* **2018**, *8*, 7113.
[19] M. M. Liu, Z. Y. Ji, X. P. Shen, H. Zhou, J. Zhu, X. L. Xie, C. S. Song, X. L. Miao, L. R. Kong, G. X. Zhu, *Eur. J. Inorg. Chem.* **2018**, *2018*,, 3952.
[20] X. Gao, G. Yu, L. Zheng, C. Zhang, H. Li, T. Wang, P. An, M. Liu, X. Qiu, W. Chen, W. Chen, *ACS Appl. Energy Mater.* **2019**, *2*, 966.
[21] T. Gao, J. Yang, M. Nishijima, H. A. Miller, F. Vizza, H. Gu, H. Chen, Y. Hu, Z. Jiang, L. Wang, L. Shuai, M. Qiu, C. Lei, A. Zhang, Y. Hou, Q. He, *J. Electrochem. Soc.* **2018**, *165*, F1147.
[22] E. Demir, S. Akbayrak, A. M. Önal, S. Özkar, *ACS Appl. Mater. Interfaces* **2018**, *10*, 6299.
[23] M. Akbayrak, A. M. Önal, *J. Electrochem. Soc.* **2019**, *166*, H897.
[24] Z. Sun, J. Zhang, J. Xie, M. Wang, X. Zheng, Z. Zhang, X. Li, B. Tang, *Dalton Trans.* **2018**, *47*, 12667.
[25] Y. Xiao, W. Wang, Q. Wu, *Int. J. Hydrogen Energy* **2020**, *45*, 3948.
[26] S. Jiang, R. Zhang, H. Liu, Y. Rao, Y. Yu, S. Chen, Q. Yue, Y. Zhang, Y. Kang, *J. Am. Chem. Soc.* **2020**, *142*, 6461.
[27] L. Xiong, J. Bi, L. Wang, S. Yang, *Int. J. Hydrogen Energy* **2018**, *43*, 20372.
[28] R. Zhang, X. Ren, S. Hao, R. Ge, Z. Liu, A. M. Asiri, L. Chen, Q. Zhang, X. Sun, *J. Mater. Chem. A* **2018**, *6*, 1985.
[29] L. Zhang, X. Ren, X. Guo, Z. Liu, A. M. Asiri, B. Li, L. Chen, X. Sun, *Inorg. Chem.* **2018**, *57*, 548.
[30] B. Zhang, H. Qin, L. Diao, N. Zhao, C. Shi, E. Liu, C. He, *J. Catal.* **2019**, *377*, 582.
[31] M. Zhao, Y. Li, H. Dong, L. Wang, Z. Chen, Y. Wang, Z. Li, M. Xia, G. Shao, *Catalysts* **2017**, *7*, 197.
[32] Z. Sun, J. Zhang, J. Xie, X. Zheng, M. Wang, X. Li, B. Tang, *Inorg. Chem. Front.* **2018**, *5*, 3042.
[33] M. Bellini, M. V. Pagliaro, A. Lenarda, P. Fornasiero, M. Marelli, C. Evangelisti, M. Innocenti, Q. Jia, S. Mukerjee, J. Jankovic, L. Wang, J. R. Varcoe, C. B. Krishnamurthy, I. Grinberg, E. Davydova, D. R. Dekel, H. A. Miller, F. Vizza, *ACS Appl. Energy Mater.* **2019**, *2*, 4999.
[34] H. Yu, E. S. Davydova, U. Ash, H. A. Miller, L. Bonville, D. R. Dekel, R. Maric, *Nano Energy* **2019**, *57*, 820.
[35] V. Yarmiayev, M. Alesker, A. Muzikansky, M. Zysler, D. Zitoun, *J. Electrochem. Soc.* **2019**, *166*, F3234.
[36] N. Ralbag, E. S. Davydova, M. Mann-Lahav, P. Cong, J. He, A. M. Beale, G. S. Grader, D. Avnir, D. R. Dekel, *J. Electrochem. Soc.* **2020**, *167*, 054514.
[37] H. A. Miller, F. Vizza, M. Marelli, A. Zadick, L. Dubau, M. Chatenet, S. Geiger, S. Cherevko, H. Doan, R. K. Pavlicek, S. Mukerjee, D. R. Dekel, *Nano Energy* **2017**, *33*, 293.
[38] H. A. Miller, A. Lavacchi, F. Vizza, M. Marelli, F. Di Benedetto, F. D. Y. AcapitoPaska I, Y. Paska, M. Page, D. R. Dekel, *Angew. Chem. Int. Ed.* **2016**, *55*, 6004.
[39] V. Men Truong, J. Richard Tolchard, J. Svendby, M. Manikandan, H. A. Miller, S. Sunde, H. Yang, D. R. Dekel, O. Barnett, *Energies* **2020**, *13*, 582.
[40] B. Qin, H. Yu, J. Chi, J. Jia, X. Gao, D. Yao, B. Yi, Z. Shao, *RSC Adv.* **2017**, *7*, 31574.
[41] J. Song, C. Wei, Z. F. Huang, C. Liu, L. Zeng, X. Wang, Z. J. Xu, *Chem. Soc. Rev.* **2020**, *49*, 2196.
[42] Y. Yang, T. Yue, Y. Wang, Z. Yang, X. Jin, *Microchem. J.* **2019**, *148*, 42.
[43] T. Li, S. Li, Q. Liu, Y. Tian, Y. Zhang, G. Fu, Y. Tang, *ACS Sustain. Chem. Eng.* **2019**, *7*, 17950.
[44] E. Demir, S. Akbayrak, A. M. Onal, S. Ozkar, *J. Colloid Interface Sci.* **2019**, *534*, 704.
[45] F. Liang, Y. Yu, W. Zhou, X. Xu, Z. Zhu, *J. Mater. Chem. A* **2015**, *3*, 634.
[46] Z. Liu, N. Li, H. Zhao, Y. Zhang, Y. Huang, Z. Yin, Y. Du, *Chem. Sci.* **2017**, *8*, 3211.
[47] G. Fang, J. Cai, Z. Huang, C. Zhang, *RSC Adv.* **2019**, *9*, 17891.
[48] Q. Wu, Q. Gao, L. Sun, H. Guo, X. Tai, D. Li, L. Liu, C. Ling, X. Sun, *Chinese J. Catal.* **2021**, *42*, 482.
[49] B. Wang, P. Xi, C. Shan, H. Chen, H. Xu, K. Iqbal, W. Liu, Y. Tang, *Adv. Mater. Interfaces* **2017**, *4*, 1700272.
[50] E. Cossar, A. Oyarce Barnett, F. Seland, E. A. Baranova, *Catalysts* **2019**, *9*, 814.
[51] L. Chen, H. Jang, M. G. Kim, Q. Qin, X. Liu, J. Cho, *Inorg. Chem. Front.* **2020**, *7*, 470.
[52] G. Liu, M. Wang, Y. Wu, N. Li, F. Zhao, Q. Zhao, J. Li, *Appl. Catal., B* **2020**, *260*, 118199.
[53] Z. Sun, X. Cao, I. G. G. Martinez, M. H. Rummeli, R. Yang, *Electrochem. Commun.* **2018**, *93*, 35.
[54] B. Qiu, C. Wang, N. Zhang, L. Cai, Y. Xiong, Y. Chai, *ACS Catal.* **2019**, *9*, 6484.
[55] J. A. Haber, E. Anzenburg, J. Yano, C. Kisielowski, J. M. Gregoire, *Adv. Energy. Mater.* **2015**, *5*, 1402307.
[56] M. Favaro, W. S. Drisdell, M. A. Marcus, J. M. Gregoire, E. J. Crumlin, J. A. Haber, J. Yano, *ACS Catal.* **2017**, *7*, 1248.
[57] L. Yang, R. Liu, L. Jiao, *Adv. Funct. Mater.* **2020**, *30*, 1909618.
[58] Y. Yu, X. Peng, U. Ali, X. Liu, Y. Xing, S. Xing, *Inorg. Chem. Front.* **2019**, *6*, 3255.
[59] Y. R. Zheng, M. R. Gao, Q. Gao, H. H. Li, J. Xu, Z. Y. Wu, S. H. Yu, *Small* **2015**, *11*, 182.
[60] X. Wu, Y. Yang, T. Zhang, B. Wang, H. Xu, X. Yan, Y. Tang, *ACS Appl. Mater. Interfaces* **2019**, *11*, 39841.
[61] J.-H. Kim, K. Shin, K. Kawashima, D. H. Youn, J. Lin, T. E. Hong, Y. Liu, B. R. Wygant, J. Wang, G. Henkelman, C. B. Mullins, *ACS Catal.* **2018**, *8*, 4257.
[62] K. Obata, K. Takanabe, *Angew. Chem. Int. Ed. Engl.* **2018**, *57*, 1616.
[63] T. Zhang, X. Wu, Y. Fan, C. Shan, B. Wang, H. Xu, Y. Tang, *ChemNanoMat* **2020**, *6*, 1119.
[64] H. Sun, C. Tian, G. Fan, J. Qi, Z. Liu, Z. Yan, F. Cheng, J. Chen, C. P. Li, M. Du, *Adv. Funct. Mater.* **2020**, *30*, 1910596.
[65] W. Peng, L. Zhao, C. Zhang, Y. Yan, Y. Xian, *Electrochim. Acta* **2016**, *191*, 669.

© 2021 The Authors. Advanced Energy and Sustainability Research published by Wiley-VCH GmbH

[66] L. Sun, L. Zhou, C. Yang, Y. Yuan, *Int. J. Hydrogen Energy* **2017**, *42*, 15140.
[67] S. Soren, I. Hota, A. K. Debnath, D. K. Aswal, K. S. K. Varadwaj, P. Parhi, *Front. Chem.* **2019**, *7*.
[68] L. Pi, R. Jiang, W. Cai, L. Wang, Y. Wang, J. Cai, X. Mao, *ACS Appl. Mater. Interfaces* **2020**, *12*, 3642.
[69] J. K. Norskov, J. Rossmeisl, A. Logadottir, L. Lindqvist, J. R. Kitchin, T. Bligaard, H. Jonsson, *J. Phys. Chem. B* **2004**, *108*, 17886.
[70] V. S. Pinheiro, F. M. Souza, T. C. Gentil, P. Böhnstedt, E. C. Paz, L. S. Parreira, P. Hammer, B. L. Batista, M. C. Santos, *ChemElectroChem* **2019**, *6*, 5124.
[71] Y. Li, X. Zhang, S. Wang, G. Sun, *ChemElectroChem* **2018**, *5*, 2442.
[72] C. Du, X. Gao, C. Cheng, Z. Zhuang, X. Li, W. Chen, *Electrochim. Acta* **2018**, *266*, 348.
[73] J. C. Carrillo-Rodríguez, S. García-Mayagoitia, R. Pérez-Hernández, M. T. Ochoa-Lara, F. Espinosa-Magaña, F. Fernández-Luqueño, P. Bartolo-Pérez, I. L. Alonso-Lemus, F. J. Rodríguez-Varela, *J. Power Sources* **2019**, *414*, 103.
[74] J. C. Carrillo-Rodriguez, S. Garcia-Mayagoitia, R. Perez-Hernandez, M. T. Ochoa-Lara, F. Espinosa-Magana, F. Fernandez-Luqeno, I. L. Alonso-Lemus, F. J. Rodriguez-Varela, *ECS Trans.*, **2017**, *77*, 1359.
[75] J. Yang, J. Wang, L. Zhu, Q. Gao, W. Zeng, J. Wang, Y. Li, *Ceram. Int.* **2018**, *44*, 23073.
[76] J. Yang, J. Wang, L. Zhu, W. Zeng, J. Wang, *Mater. Lett.* **2019**, *234*, 331.
[77] X. Wang, J. Xu, Z. Wu, M. Zhi, Z. Hong, F. Huang, *ChemNanoMat* **2019**, *5*, 831.
[78] S. Parwaiz, K. Bhunia, A. K. Das, M. M. Khan, D. Pradhan, *J. Phys. Chem. C* **2017**, *121*, 20165.
[79] A. Sivanantham, P. Ganesan, S. Shanmugam, *Appl. Catal., B* **2018**, *237*, 1148.
[80] Y. Yu, B. He, Y. Liao, X. Yu, Z. Mu, Y. Xing, S. Xing, *ChemElectroChem* **2018**, *5*, 793.
[81] X. Wang, J. Xu, M. Zhi, Z. Hong, F. Huang, *J. Alloys Compd.* **2019**, *801*, 192.
[82] M. Ji, B. He, Y. Yu, X. Yu, S. Xing, *ChemElectroChem* **2020**, *7*, 642.
[83] Y. Kang, W. Wang, J. Li, Y. Mi, H. Gong, Z. Lei, *J. Colloid Interface Sci.* **2020**, *578*, 796.
[84] L. Tao, Y. Shi, Y.-C. Huang, R. Chen, Y. Zhang, J. Huo, Y. Zou, G. Yu, J. Luo, C.-L. Dong, S. Yang, *Nano Energy* **2018**, *53*, 604.
[85] L. Chen, X. Liang, X. Li, J. Pei, H. Lin, D. Jia, W. Chen, D. Wang, Y. Li, *Nano Energy* **2020**, *73*.
[86] M. J. Paulo, R. H. D. Venancio, R. G. Freitas, E. C. Pereira, A. C. Tavares, *J. Electroanal. Chem.* **2019**, *840*, 367.
[87] Y.-Y. Feng, H.-S. Hu, G.-H. Song, S. Si, R.-J. Liu, D.-N. Peng, D.-S. Kong, *J. Alloys Compd.* **2019**, *798*, 706.
[88] W. Chen, J. Xue, Y. Bao, L. Feng, *Chem. Eng. J.* **2020**, *381*, 122752.
[89] M. Sedighi, A. A. Rostami, E. Alizadeh, *Int. J. Hydrogen Energy* **2017**, *42*, 4998.
[90] H. Xu, A.-L. Wang, Y.-X. Tong, G.-R. Li, *ACS Catal.* **2016**, *6*, 5198.
[91] H. Wang, Y. Xue, B. Zhu, J. Yang, L. Wang, X. Tan, Z. Wang, Y. Chu, *Int. J. Hydrogen Energy* **2017**, *42*, 20549.
[92] F. Xie, L. Ma, M. Gan, H. He, L. Hu, M. Jiang, H. Zhang, *Appl. Surf. Sci.* **2019**, *481*, 1425.
[93] Y. Zheng, X. Zhang, Z. Zhang, Y. Li, Y. Sun, Y. Lou, X. Li, Y. Lu, *J. Rare Earths* **2018**, *36*, 974.
[94] D. V. Dao, T. D. Le, G. Adilbish, I.-H. Lee, Y.-T. Yu, *J. Mater. Chem. A* **2019**, *7*, 26996.
[95] T. Gentil, V. Pinheiro, E. Paz, F. Souza, L. Parreira, M. Santos, *J. Brazil. Chem. Soc.* **2019**.
[96] Y. Zheng, Z. Zhang, X. Zhang, H. Ni, Y. Sun, Y. Lou, X. Li, Y. Lu, *Mater. Lett.* **2018**, *221*, 301.
[97] C. Liu, L. Zhang, L. Sun, W. Wang, Z. Chen, *Int. J. Hydrogen Energy* **2020**, *45*, 8558.
[98] D. Chai, W. Wang, F. Wang, W. Jing, P. Wang, Z. Lei, *Int. J. Hydrogen Energy* **2017**, *42*, 9775.
[99] W. Li, Z. Song, X. Deng, X.-Z. Fu, J.-L. Luo, *Electrochim. Acta* **2020**, *337*.
[100] P. Salarizadeh, M. B. Askari, M. Mohammadi, K. Hooshyari, *J. Phys. Chem. Solids* **2020**, *142*, 109442.
[101] G. Valenti, M. Melchionna, T. Montini, A. Boni, L. Nasi, E. Fonda, A. Criado, A. Zitolo, S. Voci, G. Bertoni, M. Bonchio, P. Fornasiero, F. Paolucci, M. Prato, *ACS Appl. Energy Mater.* **2020**, *3*, 8509, https://doi.org/10.1002/cssc.202002133.
[102] J. Fu, D. Ren, M. Xiao, K. Wang, Y. Deng, D. Luo, J. Zhu, G. Wen, Y. Zheng, Z. Bai, L. Yang, Z. Chen, *ChemSusChem* **2020**.
[103] S. B. Varandili, J. Huang, E. Oveisi, G. L. De Gregorio, M. Mensi, M. Strach, J. Vavra, C. Gadiyar, A. Bhowmik, R. Buonsanti, *ACS Catal.* **2019**, *9*, 5035.
[104] D. Wu, C. Dong, D. Wu, J. Fu, H. Liu, S. Hu, Z. Jiang, S. Z. Qiao, X.-W. Du, *J. Mater. Chem. A* **2018**, *6*, 9373.
[105] Q. Zhang, J. Du, A. B. He, Z. H. Liu, C. Y. Tao, *J. Solid State Chem.* **2019**, *279*, 9.
[106] B. Xu, L. Xia, F. Zhou, R. Zhao, H. Chen, T. Wang, Q. Zhou, Q. Liu, G. Cui, X. Xiong, F. Gong, X. Sun, *ACS Sustain. Chem. Eng.* **2019**, *7*, 2889.
[107] H. Xie, Q. Geng, X. Li, T. Wang, Y. Luo, A. A. Alshehri, K. A. Alzahrani, B. Li, Z. Wang, J. Mao, *Chem Commun.* **2019**, *55*, 10717.
[108] S. Zhang, C. Zhao, Y. Liu, W. Li, J. Wang, G. Wang, Y. Zhang, H. Zhang, H. Zhao, *Chem Commun.* **2019**, *55*, 2952.
[109] H. Xie, H. Wang, Q. Geng, Z. Xing, W. Wang, J. Chen, L. Ji, L. Chang, Z. Wang, J. Mao, *Inorg. Chem.* **2019**, *58*, 5423.
[110] S. J. Li, D. Bao, M. M. Shi, B. R. Wulan, J. M. Yan, Q. Jiang, *Adv. Mater.* **2017**, *29*, 1606550.
[111] C. Lv, C. Yan, G. Chen, Y. Ding, J. Sun, Y. Zhou, G. Yu, *Angew. Chem. Int. Ed.* **2018**, *57*, 6073.
[112] J. Qi, L. Gao, F. Wei, Q. Wan, S. Lin, *ACS Appl. Mater. Interfaces* **2019**, *11*, 47525.
[113] N. R. Manwar, A. A. Chilkalwar, K. K. Nanda, Y. S. Chaudhary, J. Subrt, S. S. Rayalu, N. K. Labhsetwar, *ACS Sustain. Chem. Eng.* **2016**, *4*, 2323.
[114] Z. Cheng, F. Wang, T. A. Shifa, C. Jiang, Q. Liu, J. He, *Small* **2017**, *13*, 1702163.
[115] B. Dong, L. Li, Z. Dong, R. Xu, Y. Wu, *Int. J. Hydrogen Energy* **2018**, *43*, 5275.
[116] A. Krishnan, S. Beena, M. Chandran, *Mater. Today: Proc.* **2019**, *18*, 4968.
[117] N.-C. Zheng, T. Ouyang, Y. Chen, Z. Wang, D.-Y. Chen, Z.-Q. Liu, *Catal. Sci. Technol.* **2019**, *9*, 1357.
[118] Y. Ma, Y. Bian, Y. Liu, A. Zhu, H. Wu, H. Cui, D. Chu, J. Pan, *ACS Sustain. Chem. Eng.* **2018**, *6*, 2552.
[119] S. Sultana, S. Mansingh, M. Scurrell, K. M. Parida, *Inorg. Chem.* **2017**, *56*, 12297.
[120] J. Qian, Z. Chen, H. Sun, F. Chen, X. Xu, Z. Wu, P. Li, W. Ge, *ACS Sustain. Chem. Eng.* **2018**, *6*, 9691.
[121] J. Qian, Z. Chen, F. Chen, Y. Wang, Z. Wu, W. Zhang, Z. Wu, P. Li, *Inorg. Chem.* **2018**, *57*, 14532.
[122] G. Swain, S. Sultana, B. Naik, K. Parida, *ACS Omega* **2017**, *2*, 3745.
[123] M. Sridharan, P. Kamaraj, Y. S. Huh, S. Devikala, M. Arthanareeswari, J. A. Selvi, E. Sundaravadivel, *Catal. Sci. Technol.* **2019**, *9*, 3686.
[124] Y. Wang, X. Hao, L. Zhang, Y. Li, Z. Jin, *Energy Fuels* **2020**, *34*, 2599.
[125] X. Cui, Z. Liu, G. Li, M. Zhang, Y. Song, J. Wang, *Int. J. Hydrogen Energy* **2019**, *44*, 23921.
[126] X. Liu, L. He, X. Chen, L. Du, X. Gu, S. Wang, M. Fu, F. Dong, H. Huang, *Int. J. Hydrogen Energy* **2019**, *44*, 16154.
[127] M. Waqas, B. Yang, L. Cao, X. Zhao, W. Iqbal, K. Xiao, C. Zhu, J. Zhang, *Catal. Sci. Technol.* **2019**, *9*, 5322.

© 2021 The Authors. Advanced Energy and Sustainability Research published by Wiley-VCH GmbH

[128] C. Zhu, Y. Wang, Z. Jiang, F. Xu, Q. Xian, C. Sun, Q. Tong, W. Zou, X. Duan, S. Wang, *Appl. Catal., B* **2019**, *259*, 118072.
[129] H. Yu, J. Xu, C. Yin, Z. Liu, Y. Li, *J. Solid State Chem.* **2019**, *272*, 102.
[130] M. Li, L. Zhang, M. Wu, Y. Du, X. Fan, M. Wang, L. Zhang, Q. Kong, J. Shi, *Nano Energy* **2016**, *19*, 145.
[131] Z. Han, Y. Yu, W. Zheng, Y. Cao, *New J. Chem.* **2017**, *41*, 9724.
[132] M. Liang, T. Borjigin, Y. Zhang, B. Liu, H. Liu, H. Guo, *Appl. Catal. B* **2019**, *243*, 566.
[133] M. Wang, M. Shen, X. Jin, J. Tian, M. Li, Y. Zhou, L. Zhang, Y. Li, J. Shi, *ACS Catal.* **2019**, *9*, 4573.
[134] H. Wang, J. Guan, J. Li, X. Li, C. Ma, P. Huo, Y. Yan, *Appl. Surf. Sci.* **2020**, *506*, 144931.
[135] P. Seeharaj, P. Kongmun, P. Paiplod, S. Prakobmit, C. Sriwong, P. Kim-Lohsoontorn, N. Vittayakorn, *Ultrason. Sonochem.* **2019**, *58*, 104657.
[136] J. Zheng, Z. Zhu, G. Gao, Z. Liu, Q. Wang, Y. Yan, *Catal. Sci. Technol.* **2019**, *9*, 3788.
[137] J. Guan, H. Wang, J. Li, C. Ma, P. Huo, *J. Taiwan. Inst. Chem. E.* **2019**, *99*, 93.
[138] Y. Wang, X. Bai, F. Wang, S. Kang, C. Yin, X. Li, *J. Hazard. Mater.* **2019**, *372*, 69.
[139] B. Huang, R. Gillen, J. Robertson, *J. Phys. Chem. C* **2014**, *118*, 24248.
[140] X. Cai, K. Chen, X. Gao, C. Xu, M. Sun, G. Liu, X. Guo, Y. Cai, B. Huang, J. Deng, J. Z. Liu, A. Tricoli, N. Wang, C. Dwyer, Y. Zhu, *Chem. Mater.* **2019**, *31*, 5769.
[141] J. Xia, H. Zhao, B. Huang, L. Xu, M. Luo, J. Wang, F. Luo, Y. Du, C. H. Yan, *Adv. Funct. Mater.* **2020**, *30*, 1908367.
[142] S. Bai, F. Liu, B. Huang, F. Li, H. Lin, T. Wu, M. Sun, J. Wu, Q. Shao, Y. Xu, X. Huang, *Nat Commun* **2020**, *11*, 954.
[143] D. Tian, K. Li, Y. Wei, X. Zhu, C. Zeng, X. Cheng, Y. Zheng, H. Wang, *Phys. Chem. Chem. Phys.* **2018**, *20*, 11912.
[144] R. Bose, K. Karuppasamy, H. Rajan, D. B. Velusamy, H.-S. Kim, A. Alfantazi, *ACS Sustain. Chem. Eng.* **2019**, *7*, 16392.

Qingqing Li received his B.S. degree from Taiyuan University of Technology in 2016 and his M.S. in chemical engineering from Guangzhou Institute of Energy Conversion, Chinese Academy of Science. Then, he joined Prof. Feng Luo and Prof. Yaping Du's group as a Ph.D. candidate. He currently works on rare-earth based electrocatalysis.

Bolong Huang received Ph.D. in 2012 from University of Cambridge, and he obtained B.Sc. from Peking University in 2007. Following a systematic training period as research assistant in Peking University and Hong Kong, he is now an assistant Professor in the Hong Kong Polytechnic University. His main research fields are DFT calculations on rare earth functional nanomaterials, defect theory of solid functional nanomaterials, DFT calculation development based on ab initio electronic self-energy corrections, and semicore orbital corrections as an implement in time-dependent DFT theory.

Yaping Du is a full professor at the School of Materials Science and Engineering, Nankai University and the director of Tianjin Key Lab for Rare Earth Materials and Applications. His research interests focus on rare-earth functional materials, and colloidal inorganic nanocrystals, and energy storage and conversion materials. In 2004, he received his B.S. degree from Lanzhou University, and in 2009, he received his Ph.D. degree from Peking University.

Chun-Hua Yan received his Ph.D. from Peking University at 1988. He was elected as a Member of the Chinese Academy of Sciences in 2011, and a Fellow of the Academy of Sciences for the Developing World (TWAS) in 2012. He is the president of Lanzhou University and the director of the State Key Laboratory of Rare Earth Materials Chemistry and Applications at Peking University, and the Centre for Rare Earth and Inorganic Functional Materials at Nankai University.

© 2021 The Authors. Advanced Energy and Sustainability Research published by Wiley-VCH GmbH